Truncated perfect hypercube fermions and overlap-hypercube fermions

Wolfgang Bietenholz, Universidad Nacional Autónoma de México

- **Perfect lattice fermions**
- **Truncation to the hypercube fermion (HF)**
- **Chiral correction to the overlap-HF**

  Scaling, locality, approximate rotation symmetry, condition number

  Applications to topology, Random Matrix Theory, Low Energy Constants

Block Variable Renomalization Group Transformation (RGT)

Integrate out field variables on a fine lattice $\rightarrow$ action on a coarser lattice represents identical physics (if the integration is carried out exactly).

Changes resolution, $i.e.$ energy level, in particular correlation length ξ in lattice units

At $\xi = \infty$: iterations may lead to a **Fixed Point Action (FPA)**

Invariant under change of lattice spacing

Leave FPA by RGTs in a relevant direction: no irrelevant lattice artifacts come in $\rightarrow$ yields continuum physics on the lattice, **perfect lattice action**

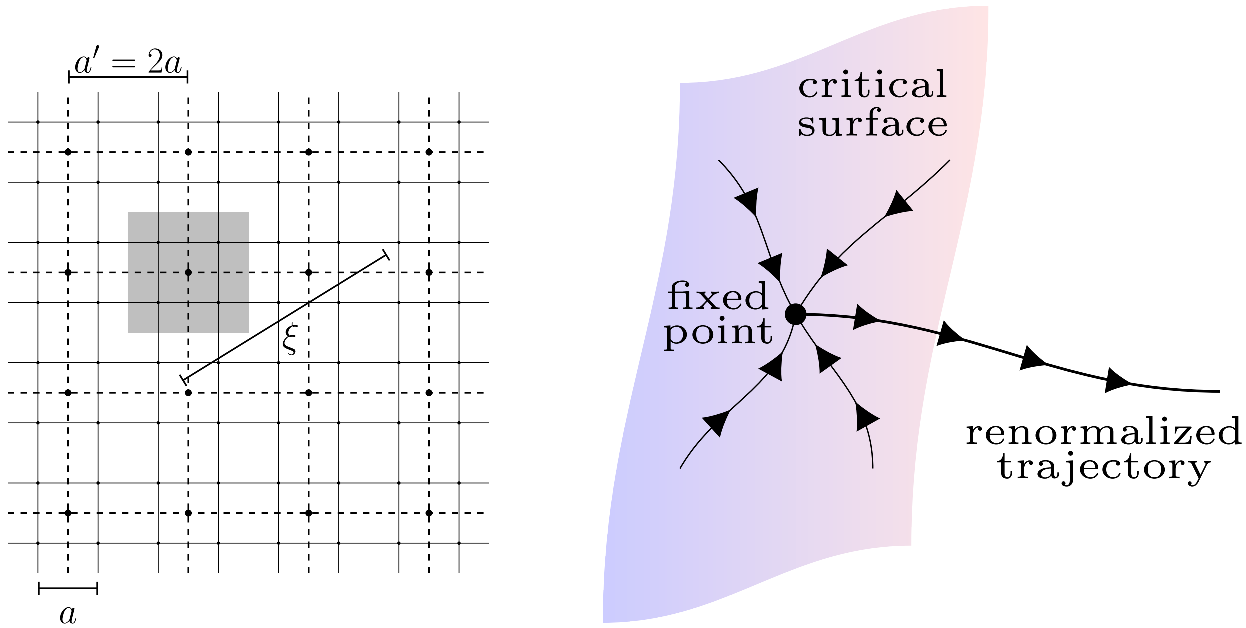

Left: Block factor 2 RGT: Average of the field values over the 2^d sites within a block (shaded) on the fine lattice (spacing a) $\rightarrow$ field value at the block center on the coarse lattice (spacing $a' = 2a$). Correlation length ξ unchanged in physical units, reduced by a factor of 2 in units of a'.

Right: Critical surface ($\xi/a = \infty$) in space of couplings. Iterated RGTs in critical surface may converge to a Fixed Point. A **renormalized trajectory** leaves the critical surface in a relevant direction: formulations free of any lattice artifacts, even at finite ξ/a — **perfect lattice actions**

[Figure from: WB/Wiese, "Quantum Field Theory and the Standard Model of Particle Physics: From Fundamental Concepts to Dynamical Mechanisms", Cambridge University Press, 2023]

Perfect action: can be computed analytically for free fermions

$$e^{-S'[\bar{\Psi},\Psi]} = \int D\bar{\psi} D\psi \, \exp\left[-S[\bar{\psi},\psi] + \frac{\rho}{2}\Big(\bar{\Psi}_x - \frac{\beta_n}{b^d}\sum_{y\in c_x}\bar{\psi}_y\Big)\Big(\Psi_x - \frac{\beta_n}{b^d}\sum_{y\in c_x}\psi_y\Big)\right]$$

x: sites on coarse lattice, y: sites on fine lattice
c_x: coarse unit hypercube associated with x
b: block size, $\beta_n = n^{(d-1)/2}$ re-scaling factor

$\bar{\psi}$, ψ: fermion fields on the fine lattice
$\bar{\Psi}$, Ψ: fermion fields on the coarse lattice

RGT: $S \to S' \to S'' \to S''' \ldots$

ρ: RGT parameter

$\rho \to \infty$: δ-blocking, but any ρ works, even $\rho_{x,x'}$, if ρ^{-1} is local

Size b of the blocking cell c_x can also be varied. Most efficient: $b \to \infty$, **blocking from the continuum** to the lattice.
Leads directly to a **perfect action for free fermions:**

$$
\begin{aligned}
S_{\rm perf}[\bar{\Psi}, \Psi] &= \sum_{x,r} \bar{\Psi}_x D_{\rm perf}(r) \Psi_{x+r} \\
&= \frac{1}{(2\pi)^d} \int_B d^d p \; \bar{\Psi}(-p) D_{\rm perf}(p) \Psi(p) \\
D^{-1}_{\rm perf}(p) &= \sum_{l \in \mathbb{Z}^d} \frac{\Pi(p + 2\pi l)^2}{\mathrm{i}\gamma_\mu (p_\mu + 2\pi l_\mu) + m} + \frac{2}{\rho} \, , \quad \Pi(p) := \prod_\mu \frac{\frac{2}{a} \sin \frac{a p_\mu}{2}}{p_\mu}
\end{aligned}
$$

[Ginsparg/Wilson '82, WB/Wiese '95, '96]   Relevant parameter: mass m

$\rho \to \infty$: chirality as in the continuum, $\{ D_{\rm perf}(m=0), \gamma_5 \} = 0$,
no doublers, how about Nielsen-Ninomiya Theorem?

Answer: $D_{\rm perf}(m=0)|_{\alpha=\infty} = D_{\rm FPA}(r)|_{\alpha=\infty} \sim |r|^{1-d}$ **non-local**

ρ finite:

$$D_{\rm perf}(r) := \rho_\mu(r)\gamma_\mu + \lambda(r)$$

Local: vector term $|\rho_\mu(r)|$ and scalar term $|\lambda(r)|$ fall off **exponentially**

$\lambda(r) \neq 0$: lattice modified chiral symmetry, fulfills
Ginsparg-Wilson relation (GW '82)

$$\{D_{\rm FPA}, \gamma_5\} = \frac{1}{\rho} D_{\rm FPA} \gamma_5 D_{\rm FPA}$$

Conceptually okay, but <u>application requires short-ranged truncation</u>

Truncation scheme: periodic boundary conditions in the hypercube with $|r_\mu| \leq 1 \;\Rightarrow$ normalized **hypercube-fermion (HF)** (couplings to 3^d sites, structure like "Brillouin fermions")

r	$\rho_1(r)$	$\lambda(r)$
$(0,0,0,0)$	0	1.85272055
$(1,0,0,0)$	0.13684679	-0.06075787
$(1,1,0,0)$	0.03207728	-0.03003603
$(1,1,1,0)$	0.01105813	-0.015967620
$(1,1,1,1)$	0.00474899	-0.008426812
$(0,0)$	0	1.48954496
$(1,0)$	0.30938846	-0.24477248
$(1,1)$	0.09530577	-0.12761376

Couplings of the free, massless HF in $d=4$ *and* $d=2$*:* $\rho_\mu(r)$ *is odd in* r_μ *and even in all other* r_ν*, while* $\lambda(r)$ *is even in all directions.*

$\rho = 1$ (in lattice units): optimized locality

Fermion mass $m=0$ is the worst case. $m>0$ accelerates exponential decay, truncation less harmful, $\rho = m^2/(2(e^m - m - 1))$

[WB/Brower/Chandrasekharan/Wiese '97]

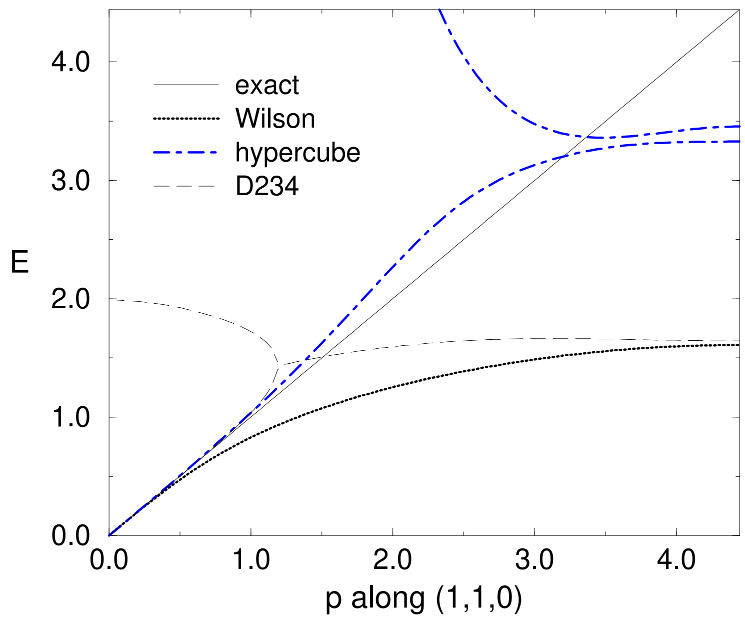

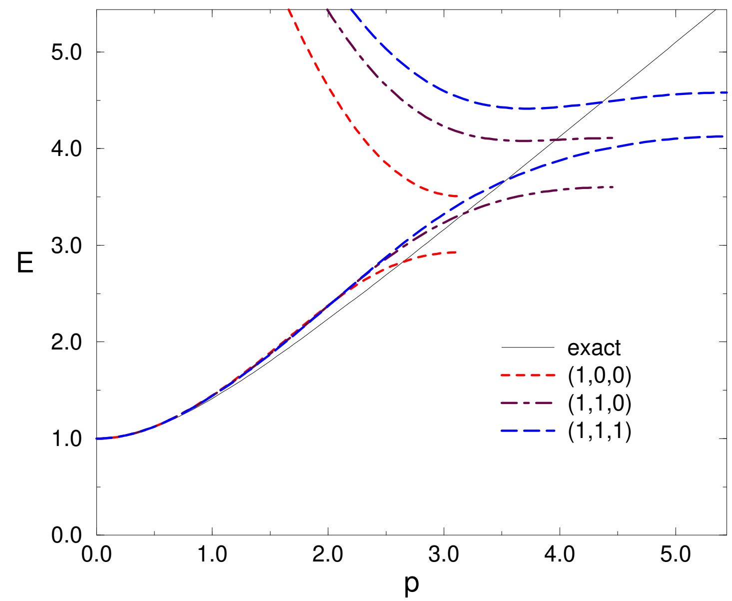

Left: Dispersion relation for free, massless 4d lattice fermions, for spatial momenta $\vec{p} \propto (1,1,0)$ (as an example). For perfect fermion: coincides with continuum dispersion; HF dispersion follows it closely. Wilson fermion deviates strongly; the Symanzik improved D234 [Alford/Klassen/Lepage '96] fermion behaves well up to $|\vec{p}\,| \approx 1$, before it hits a doubler coming down from higher energy.

Right: Dispersion relation for the free HF with mass $m = 1$. Energy $E(\vec{p})$ for various directions of $\vec{p}$ $(p = |\vec{p}\,|)$: they all follow closely the continuum dispersion over a large part of the Brillouin zone.

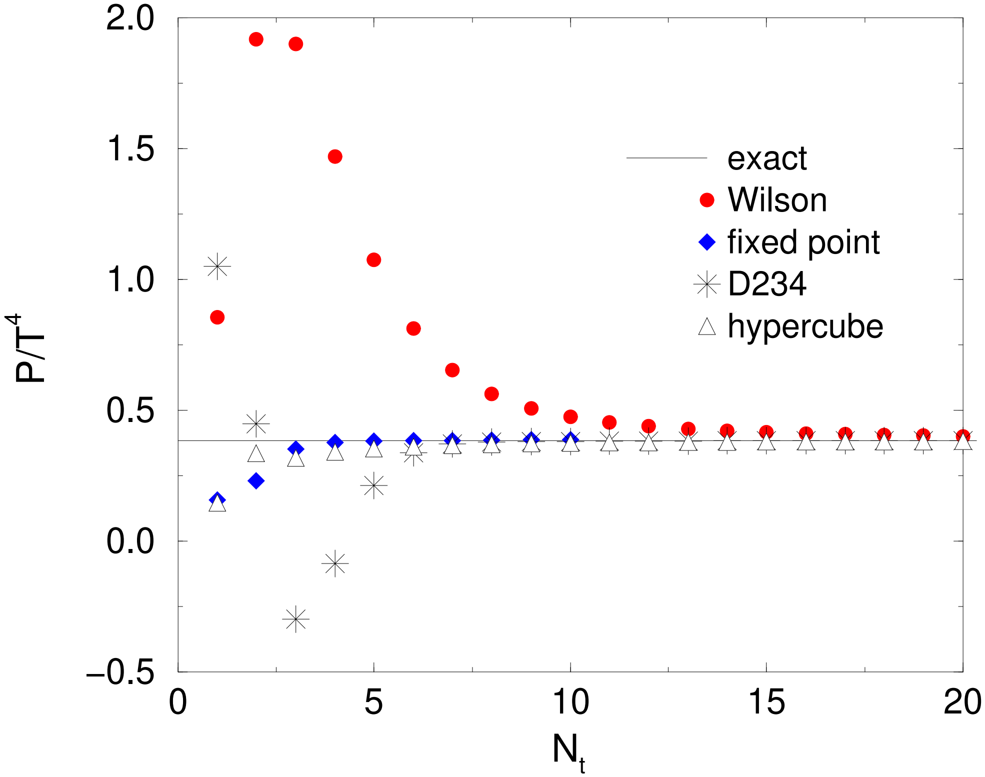

Pressure P / (temperature $T)^4$ for various types of free lattice fermions. Continuum: Stefan-Boltzmann law $P/T^4 = 7\pi^2/180$.

RGT improved actions converge much faster for decreasing temperature (increasing N_t) than the Wilson action or the D234 action.

(Here even the Fixed Point Action has (minor) artifacts, because it is constructed at $T = 0$).

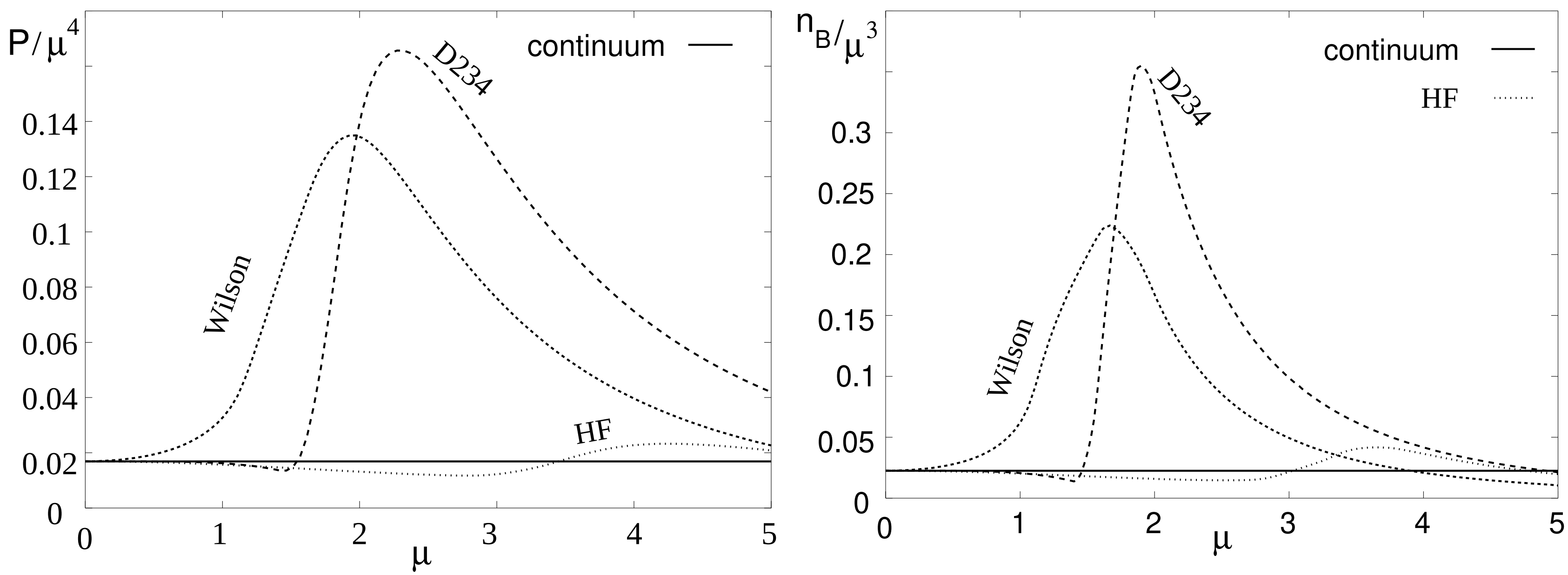

P/μ^4 and n_B/μ^3, for pressure P, baryon density n_B and chemical potential μ, at zero temperature, for various types of free, massless lattice fermions.

For the HF both ratios converge rapidly to the continuum values as μ decreases, in contrast to the Wilson fermion and the D234 fermion.

Schemes for blocking from the continuum

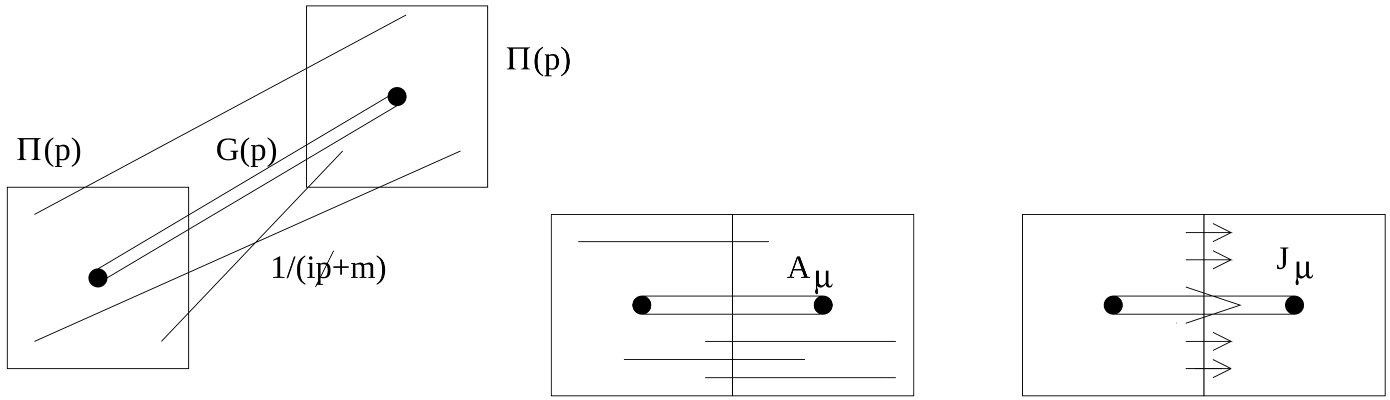

Left: **Matter fields** are blocked by integrating the continuum field in a lattice cell, with the convolution function Π. Perfect propagator G is obtained by integrating all continuum propagators between points in the corresponding lattice cells.

Center: Blocking for **non-compact gauge fields**: we integrate all straight parallel transporters between continuum points, which have the same relative position in adjacent lattice cells.

Right: Perfect **current**, obtained by integrating the continuum flux through the face between adjacent lattice cells.

Consistently perfect lattice formulation reproduces the axial anomaly

3d illustration of the HF gauging by means of **hyperlinks**

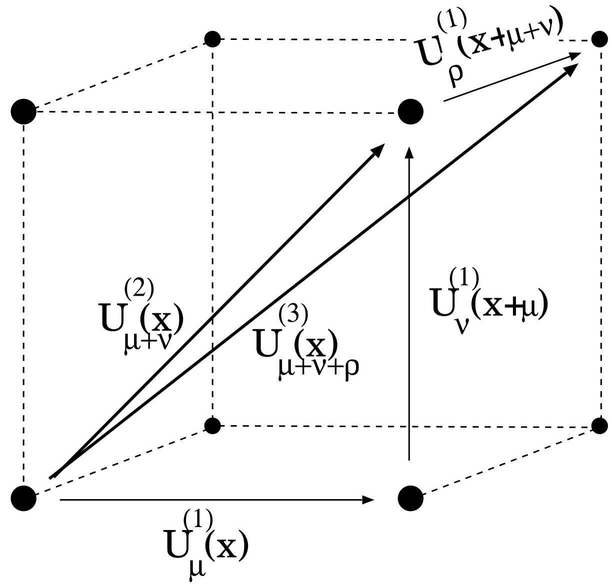

$$
\begin{aligned}
U^{(2)}_{\mu+\nu}(x) &= \frac{1}{2}\Big(\gamma_\mu U_\mu(x)\gamma_\nu U_\nu(x+a\hat{\mu}) + \gamma_\nu U_\nu(x)\gamma_\mu U_\mu(x+a\hat{\nu})\Big) \\
U^{(3)}_{\mu+\nu+\rho}(x) &= \frac{1}{6}\Big(\gamma_\nu U_\mu(x)\gamma_\nu U_\nu(x+a\hat{\mu})\gamma_\rho U_\rho(x+a\hat{\mu}+a\hat{\nu}) + \dots \\
&\quad \dots + \gamma_\rho U_\rho(x)\gamma_\nu U_\nu(x+a\hat{\rho})\gamma_\mu U_\mu(x+a\hat{\rho}+a\hat{\nu})\Big)
\end{aligned}
$$

"Rainbow preconditioning" for parallel fermion matrix inversion:
40 "colors" instead of just even/odd, successively includes more "colors"
Gain factor $3\dots 4$ [WB/Eicker/Frommer/Lippert/Medeke/Schilling/Weuffen '98]

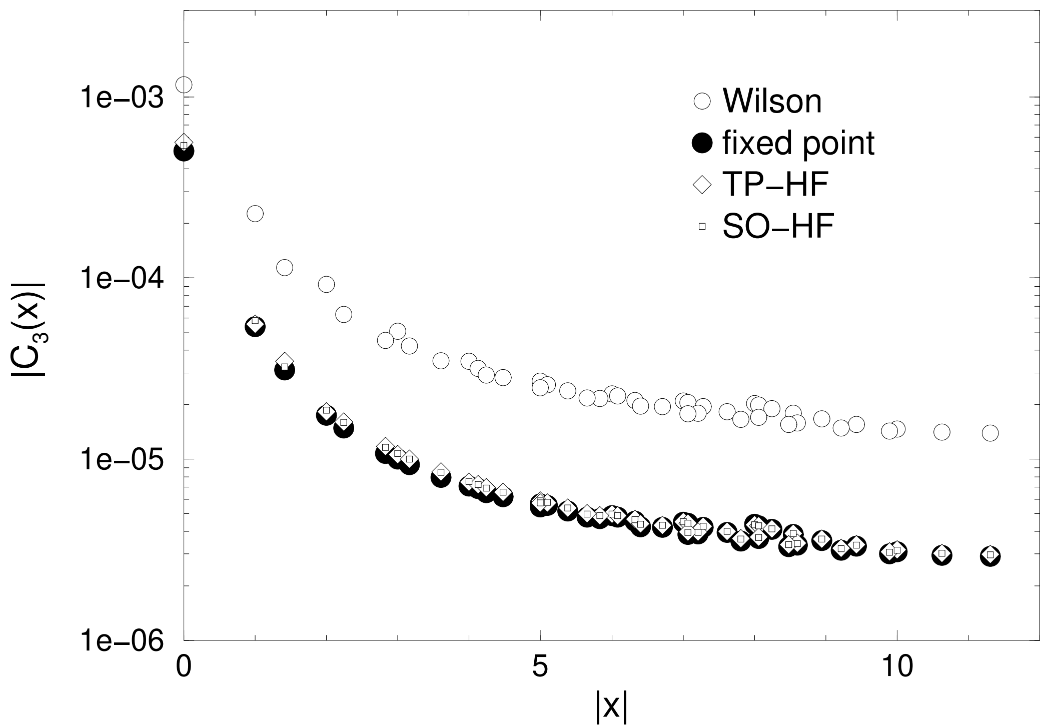

Point-to-point pseudoscalar correlation function in the 2-flavor Schwinger model for the Wilson fermion, a fixed point fermion [Lang/Pany, '98, with many terms] and two HF versions. We see in all cases but the Wilson fermion a *smooth short-range decay,* $i.e.$ **approximate rotation symmetry.**

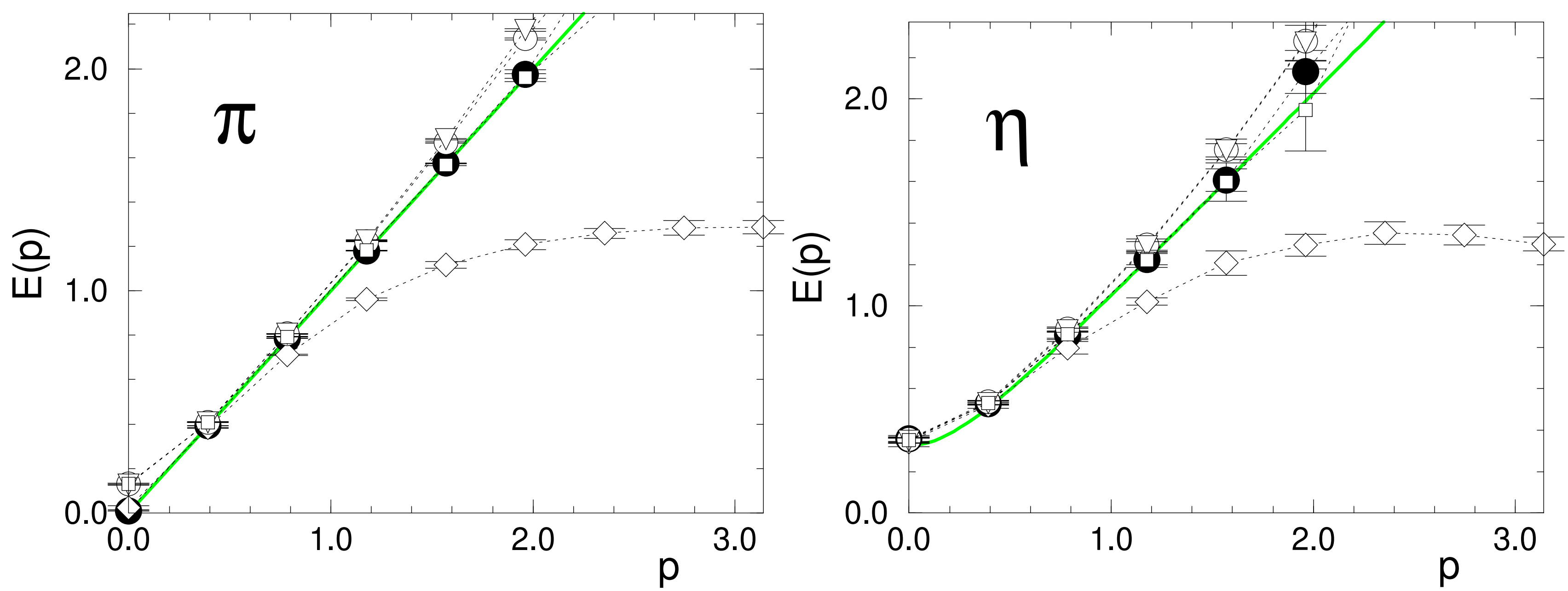

Dispersion relations for the **"pion"** and the **"η-meson"** in the 2-flavor Schwinger model: green lines: continuum; Wilson fermions (diamonds); FPA [Lang/Pany '98] (filled circles); three types of HFs, in particular the scaling optimized SO-HF (little empty boxes) performs at least as well as the FPA [WB/Hip, '00].

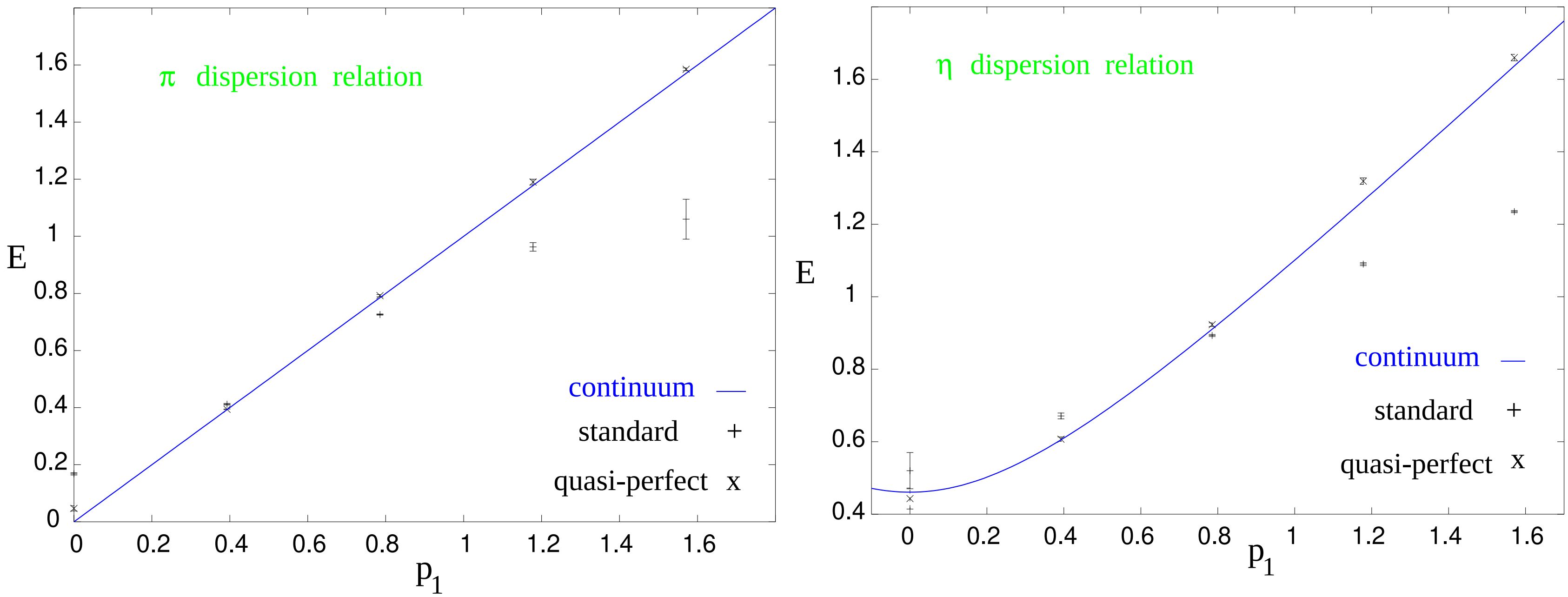

"Pion" and "η-meson" dispersion relations in the 2-flavor Schwinger model with **dynamical staggered fermions**: standard vs. truncated perfect (16×16 lattice, $m = 0$) [WB/Dilger '99], similar to HF.

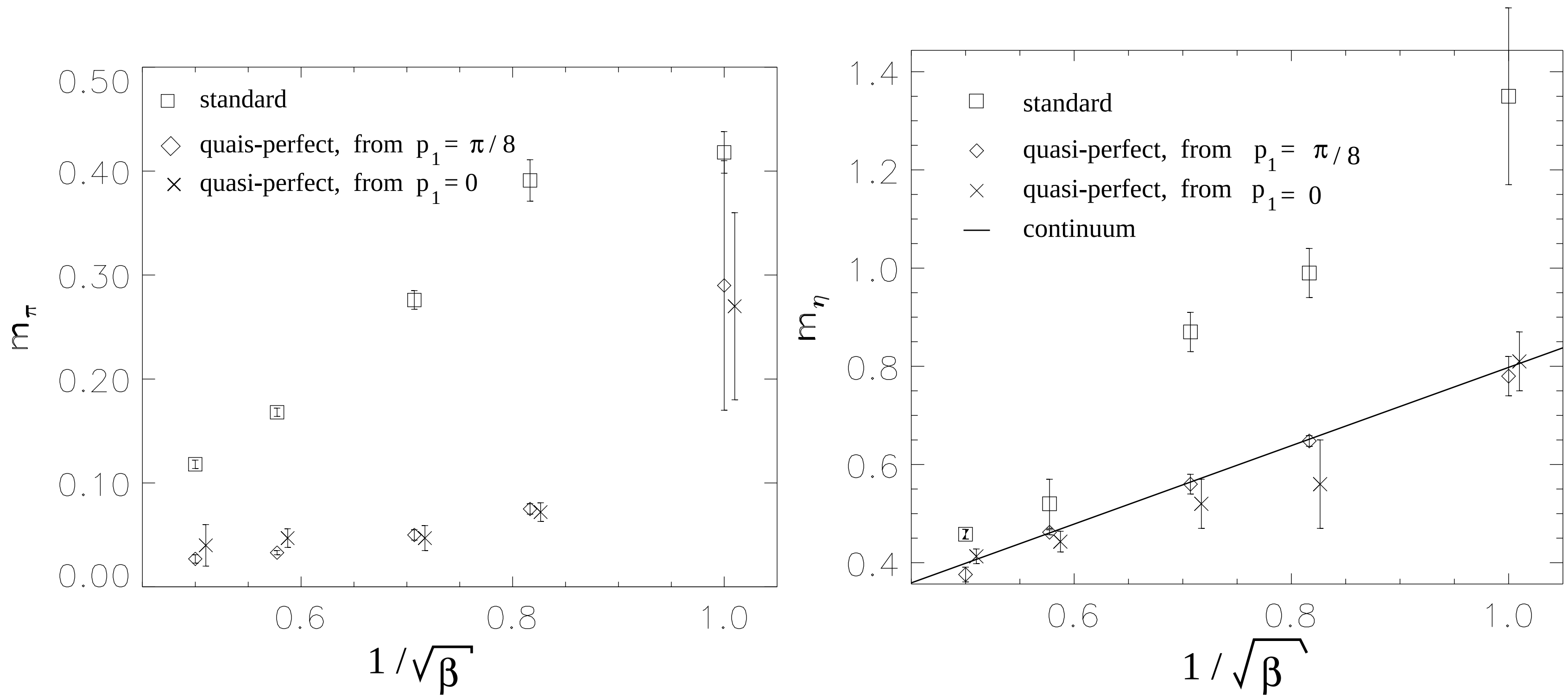

"Meson" masses in the Schwinger model with **dynamical staggered fermions**, at lattice spacings $a \propto 1/\sqrt{\beta}$. The results for the truncated perfect staggered fermion are much closer to the continuum values; in particular they provide **much lighter "pions".**

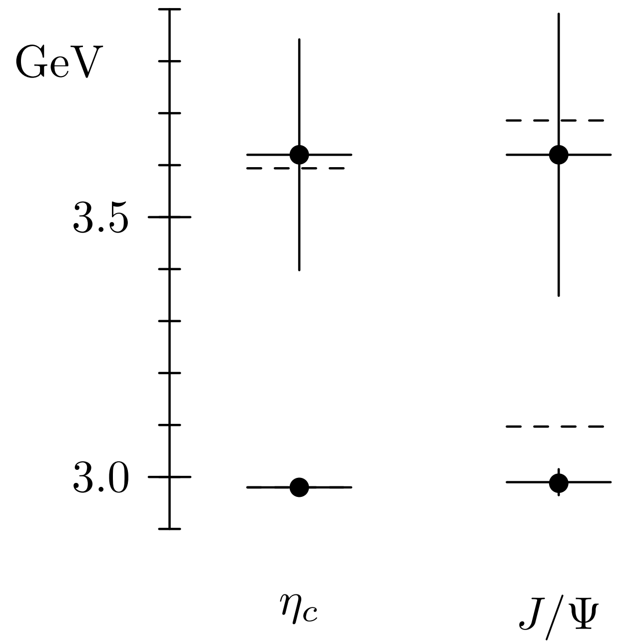

Charmonium spectrum, measured in quenched simulations with the HF and a **truncated perfect quark gluon vertex function** (rather complicated) [Orginos et al. '98].

Experimental values are dashed; the η_c ground state sets the scale.

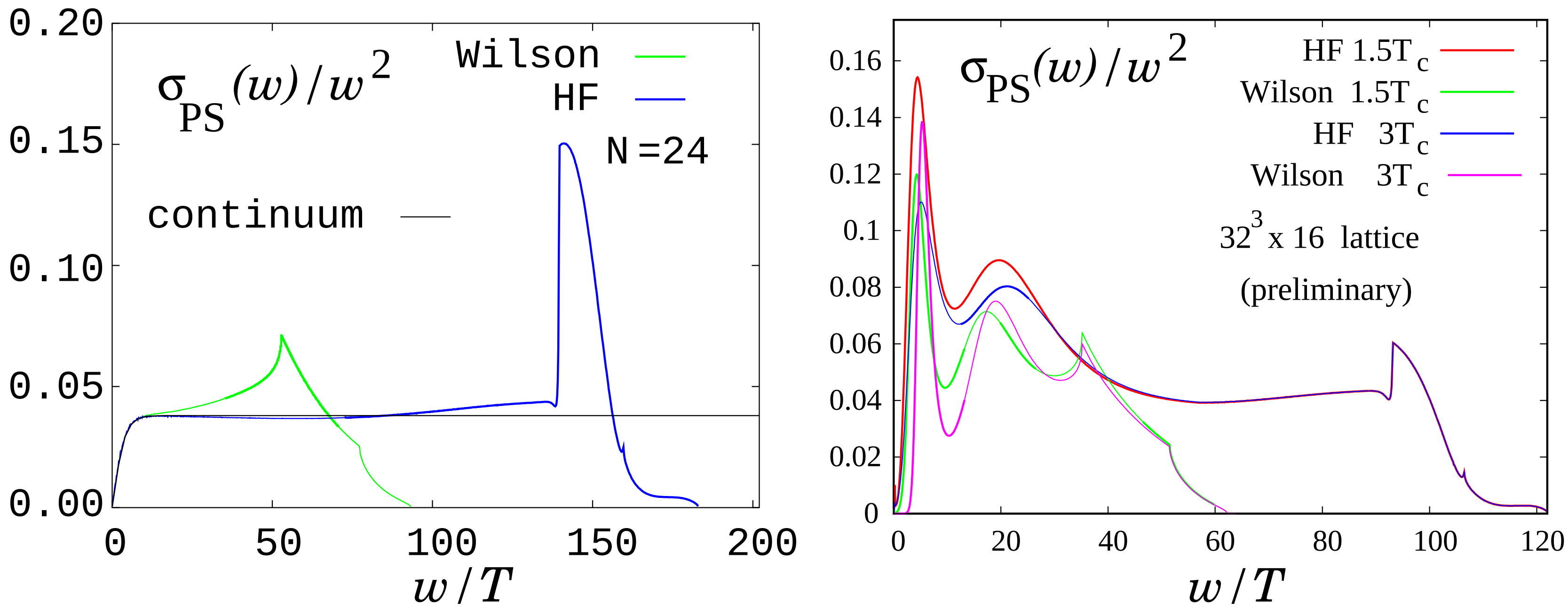

Spectral function $\sigma_{\rm PS}$, depending on the frequencies ω, at critical temperature $T_{\rm c} = \infty$ (free, left) and finite $T_{\rm c}$ (right) [Wissel, Laermann, Shcheredin, Datta, Karsch '06].

Results with the Maximum Entropy Method [Nakahara/Asakawa/Hatsuda '99].
The free HF result (left) follows the continuum up to high ω.

In both cases, the Wilson fermion result collapses at moderate ω.

$$G_\Gamma(x) = \langle J(x) J^\dagger(0)\rangle , \quad J(x) = \bar{q}(x)\Gamma q(x)$$

$$G_\Gamma(t,\vec{p}) = \int_0^\infty d\omega \; \sigma_\Gamma(\omega,\vec{p}) K(\omega,t), \quad K(\omega,t) = \cosh[\omega(t-T/2)]/\sinh(\omega/2T)$$

Ginsparg-Wilson Relation (GWR) and Overlap formula

Lattice modified chirality circumvents the Nielsen-Ninomiya Theorem (Lüscher, '98).

Set $\rho = 1$ in lattice units; local transformation

$$\begin{aligned} \bar{\Psi} D \Psi \quad &\to \quad \bar{\Psi}\Big(1 - \varepsilon(1 - \frac{1}{2}D)\gamma_5\Big) D \Big(1 + \varepsilon\gamma_5(1 - \frac{1}{2}D)\Big)\Psi + \mathcal{O}(\varepsilon^2) \\ &= \quad \bar{\Psi} D \Psi + \varepsilon\bar{\Psi}\Big[\underbrace{\{D, \gamma_5\} - D\gamma_5 D}_{=0,\ \mathrm{GWR}}\Big] + \mathcal{O}(\varepsilon^2) \end{aligned}$$

For finite ε mysterious, but not needed.

Satisfied by $D_{\mathrm{perf}}(m = 0)$ (Ginsparg/Wilson '83, Hasenfratz '97), but hard to construct and apply.

Overlap formula (Neuberger '98)

D_0: some massless lattice Dirac operator, γ_5-Hermitian: $D_0^\dagger = \gamma_5 D_0 \gamma_5$

$A := D_0 - 1$ (generally $D_0 - \rho$) is unitary, *iff* D_0 is a GW operator,

$$A^\dagger A = \gamma_5 \Big[\underbrace{D_0 \gamma_5 D_0 - \{D, \gamma_5\}}_{0} + \gamma_5 \Big] = 1$$

Usually not fulfilled, $e.g.$ for $D_0 = D_{\rm W}$, *but we can enforce it* by substituting

$$\begin{aligned} A \to A_{\rm ov} &= A/\sqrt{A^\dagger A} \quad \Rightarrow \quad A_{\rm ov}^\dagger A_{\rm ov} = 1 \\ D_{\rm ov} &= 1 + A_{\rm ov} = 1 + (D_0 - 1)/\sqrt{(D_0^\dagger - 1)(D_0 - 1)} \\ &= 1 + \gamma_5 H/\sqrt{H^2}\ , \quad H := \gamma_5 A = H^\dagger \end{aligned}$$

Overlap-Hypercube Fermion

Neuberger inserts $D_{\rm W}$, but D_0 can also be *e.g.* $D_{\rm HF}$ (WB '98, Niedermayer '99, DeGrand '00), which is already approx. chiral, in contrast to $D_{\rm W}$.

$\Rightarrow \sqrt{\dots} \approx 1$, minor chiral correction

More couplings in the kernel, *but*

- better locality $\to$ valid up to stronger gauge coupling
- preserves good scaling and approx. rotation invariance
- small condition number of $A^\dagger A$ $\to$ convergence with modest polynomial for $1/\sqrt{\dots}$

Approximate chirality of the HF

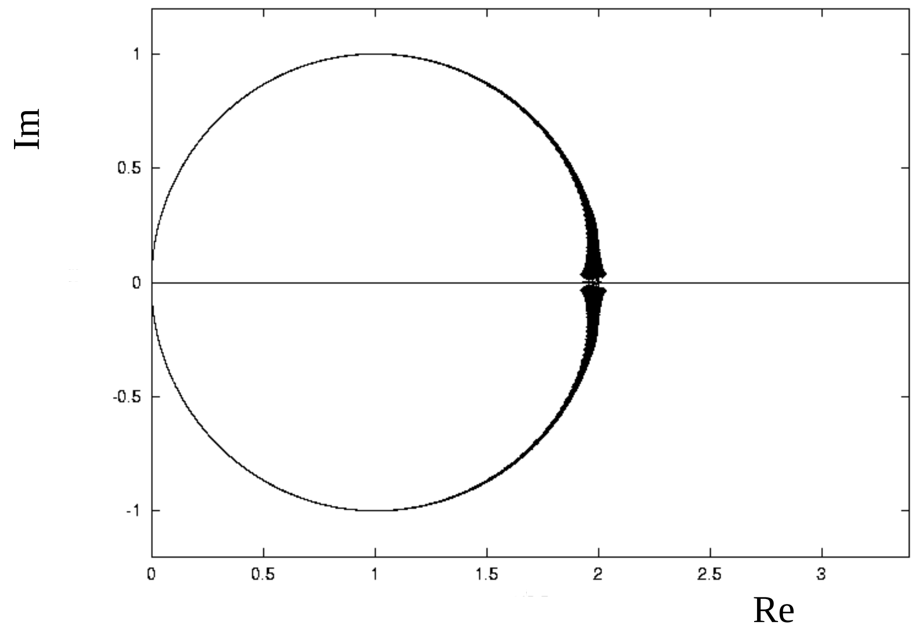

Spectrum of the free 4d HF (in infinite volume): close to GW circle with center 1 and radius 1 ($\rho = 1$): approximates chirality very well [WB '98].

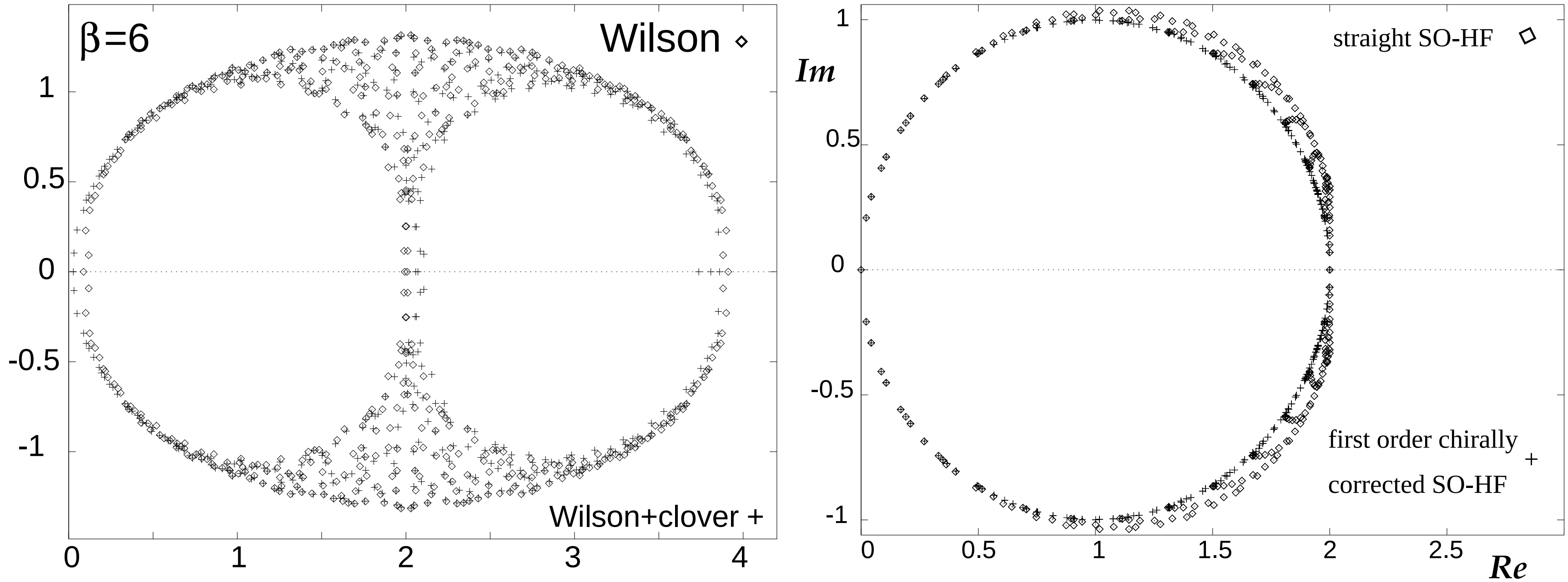

Spectra of the Wilson operator (left, without and with a clover term) and of the HF operator (right) for a typical conf. in the 2-flavor Schwinger model at $\beta = 6$. [WB/Hip '00]

The Wilson spectrum deviates strongly from the GW circle, whereas the HF spectrum approximates it well. For the HF we add a correction where the overlap formula is approximated by a *1*$^{\mathrm{st}}$ *order polynomial*, which is sufficient to put the eigenvalues quite exactly onto the GW circle.

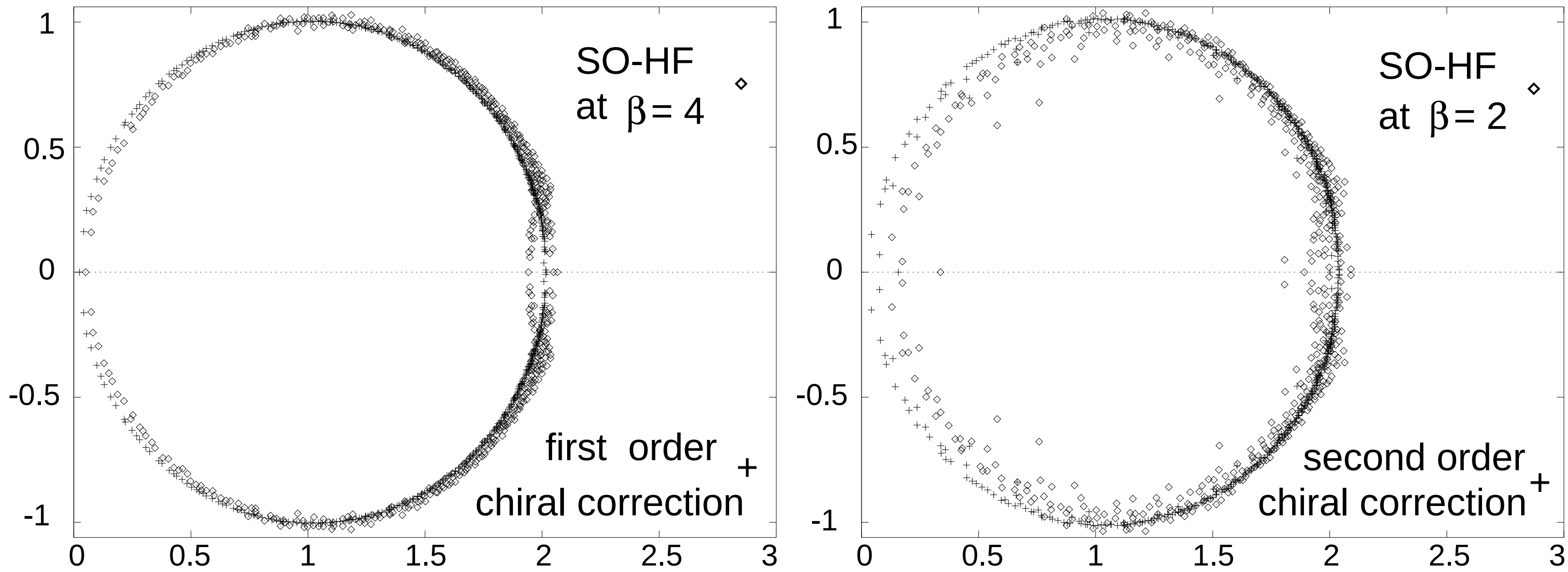

Spectra of the HF operator for typical configurations in the Schwinger model at $\beta = 4$ *and at* $\beta = 2$.

The GW circle is still approximated well. We include a polynomial correction with the Taylor expanded overlap formula to the 1^{st} and 2^{nd} order.

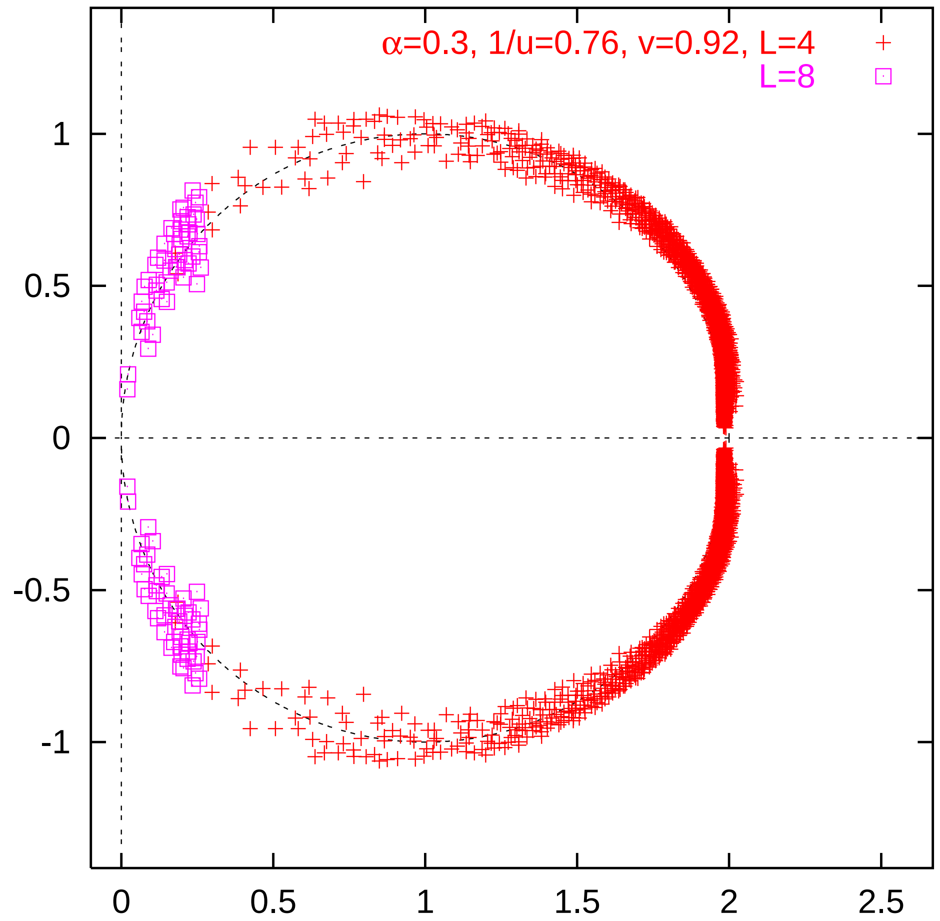

Spectrum of the optimized HF operator for a typical configuration in **quenched QCD at** $\beta = 6$ (standard gluon action) on lattices of the size 4^4 (crosses, full spectrum) and 8^4 (squares, physical part of the spectrum)

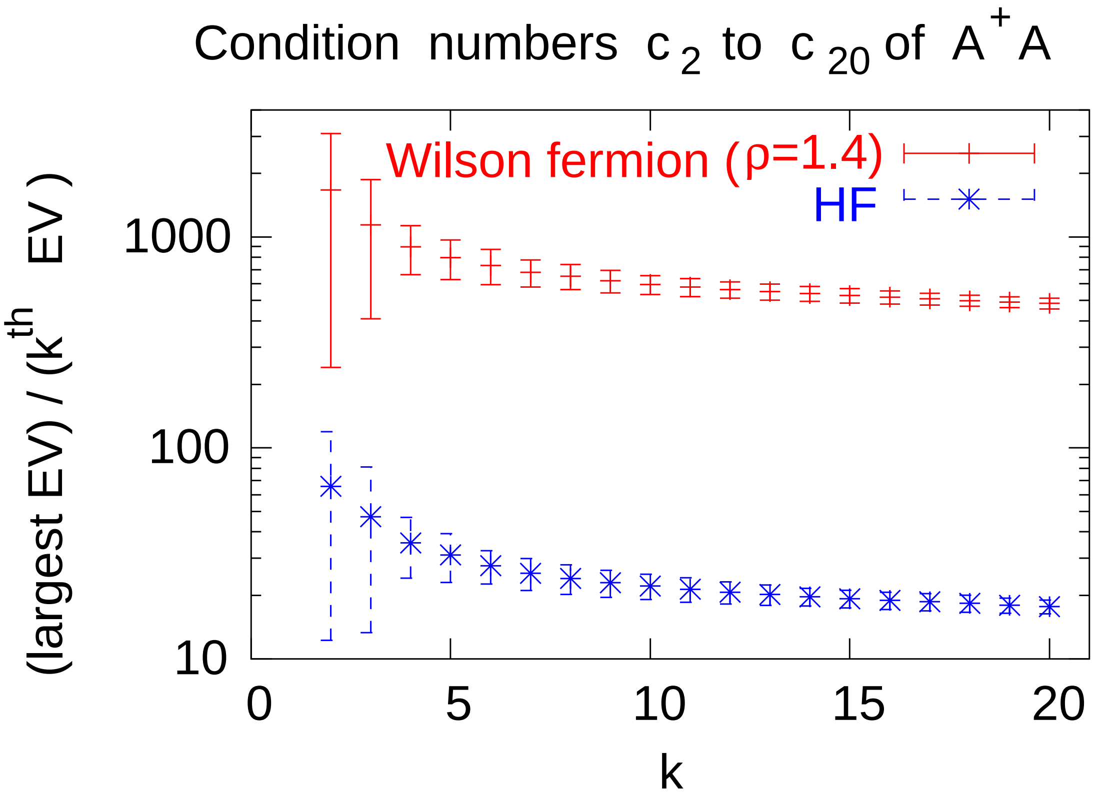

Condition numbers c_k of $A^\dagger A = H^2$, where $A = D_0 - \alpha$, for $D_0 = D_\mathrm{W}$ and $D_0 = D_\mathrm{HF}$, in QCD on a 12^4 lattice at $\beta = 6$. The $k-1$ lowest modes which are projected out. $c_k := (\text{largest eigenvalue of } A^\dagger A)/(k^\text{th} \text{ eigenvalue of } A^\dagger A)$ is ≈ 25 times lower for the HF [WB '02] $\Rightarrow$ gain factor ≈ 5 in the (polynomial degree for $1/\sqrt{A^\dagger A}$) $\propto$ computational effort.

Gain factor $\approx$ same at $\beta = 5.85$ on a $12^3 \times 24$ lattice [WB/Shcheredin '06].

Locality of overlap fermions

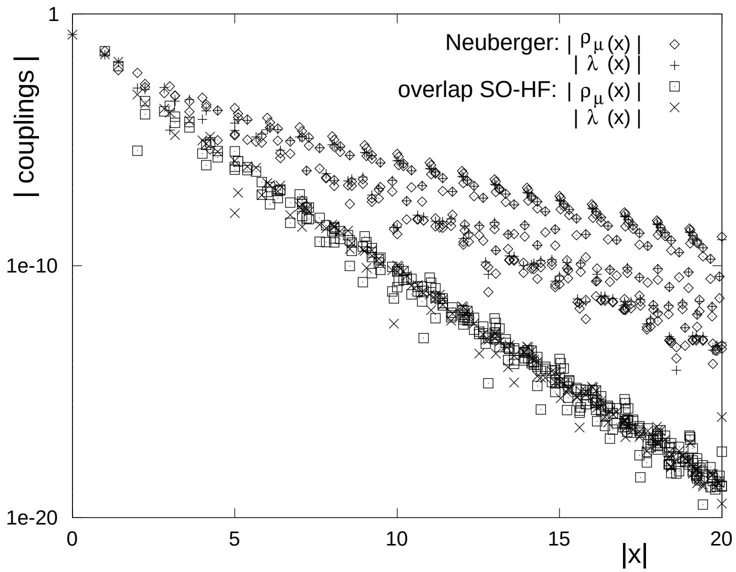

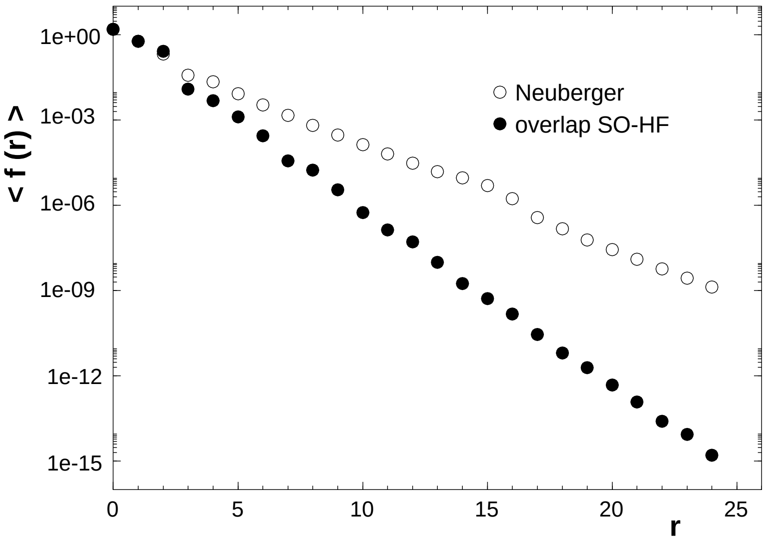

Locality of the overlap-HF vs. the Neuberger operator in $d = 2$.

Left: Decay of the free couplings of the vector term ρ_μ and scalar term λ in the Euclidean distance $|x|$. The exponential of the overlap-HF is much faster $\to$ higher level of locality.

Couplings in the Neuberger operator are much more spread out $\to$ better approximate rotation symmetry for the overlap-HF.

Right: Schwinger model at $\beta = 6$, locality measured by the largest coupling at fixed taxi driver distance [method by Hernández/Jansen/Lüscher '99]

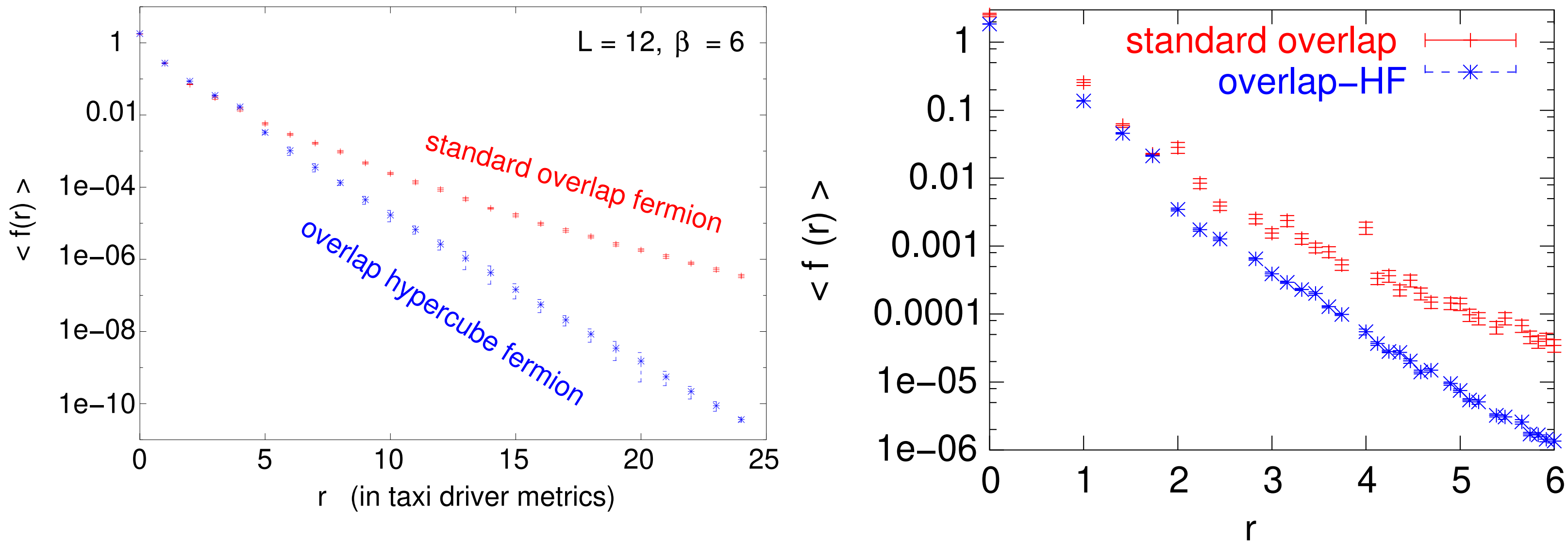

Locality of the overlap-HF vs. Neuberger operator in quenched QCD

Left: Decay in the taxi driver metrics at $\beta = 6$, the gain factor in the exponent is almost 2 in the exponent of the decay [WB '02].

Right: $\beta = 5.85$ in Euclidean metrics, which also compares the quality of rotation symmetry

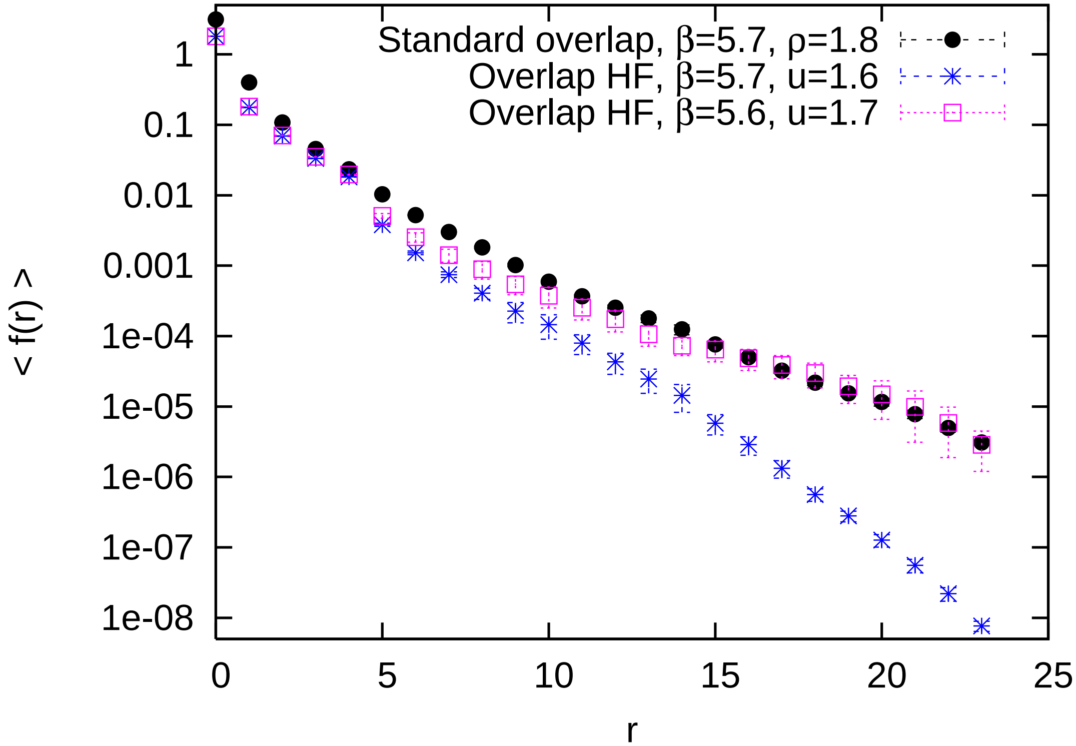

Locality of the overlap-HF (with link amplification factor u and $\alpha = 1$) vs. $D_{\rm N}$, in QCD at **strong coupling** *(taxi driver metrics).*

At $\beta = 5.7$, $D_{\rm N}$ (with optimized $\alpha = 1.8$) is still local, but at $\beta = 5.6$ its locality — and therefore its validity as a lattice Dirac operator — collapses. **The overlap-HF is local in both cases.**

Measurements on a $12^3 \times 24$ lattice, anisotropy $\to$ bending down at large r.

Scaling of overlap fermions

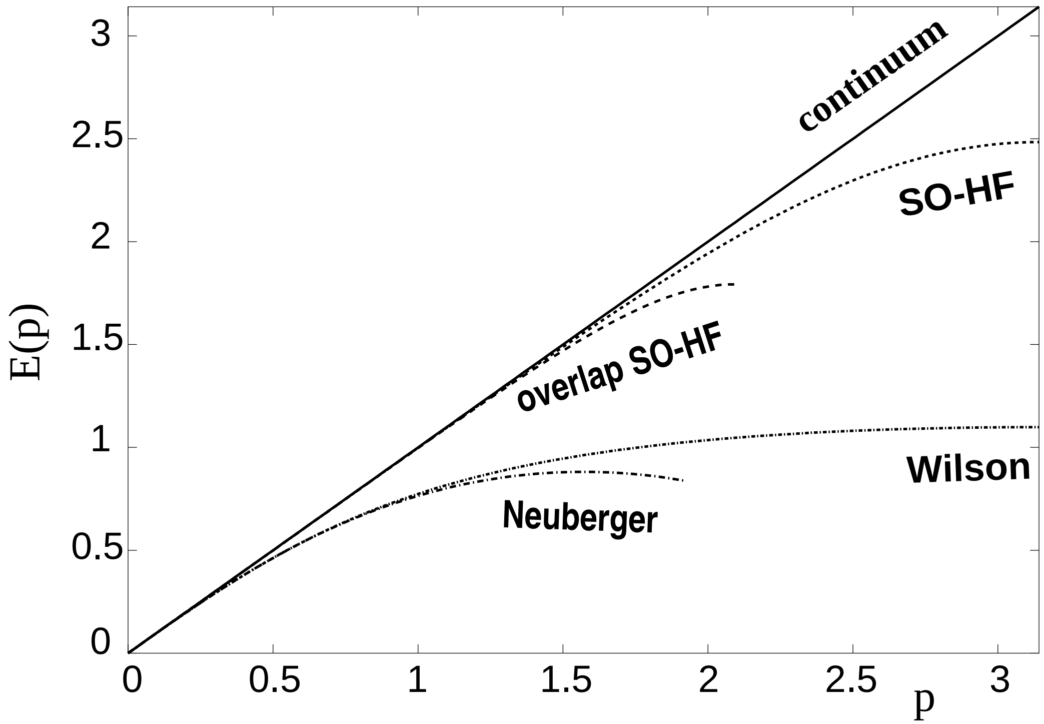

Dispersion relation of the free, massless 2d (scaling optimized) overlap-HF, compared to the continuum and to D_{N}*.*

The dispersions end when the argument of the square root becomes negative.

For an overview, we include the dispersion for the kernels D_{HF} and D_{W}.

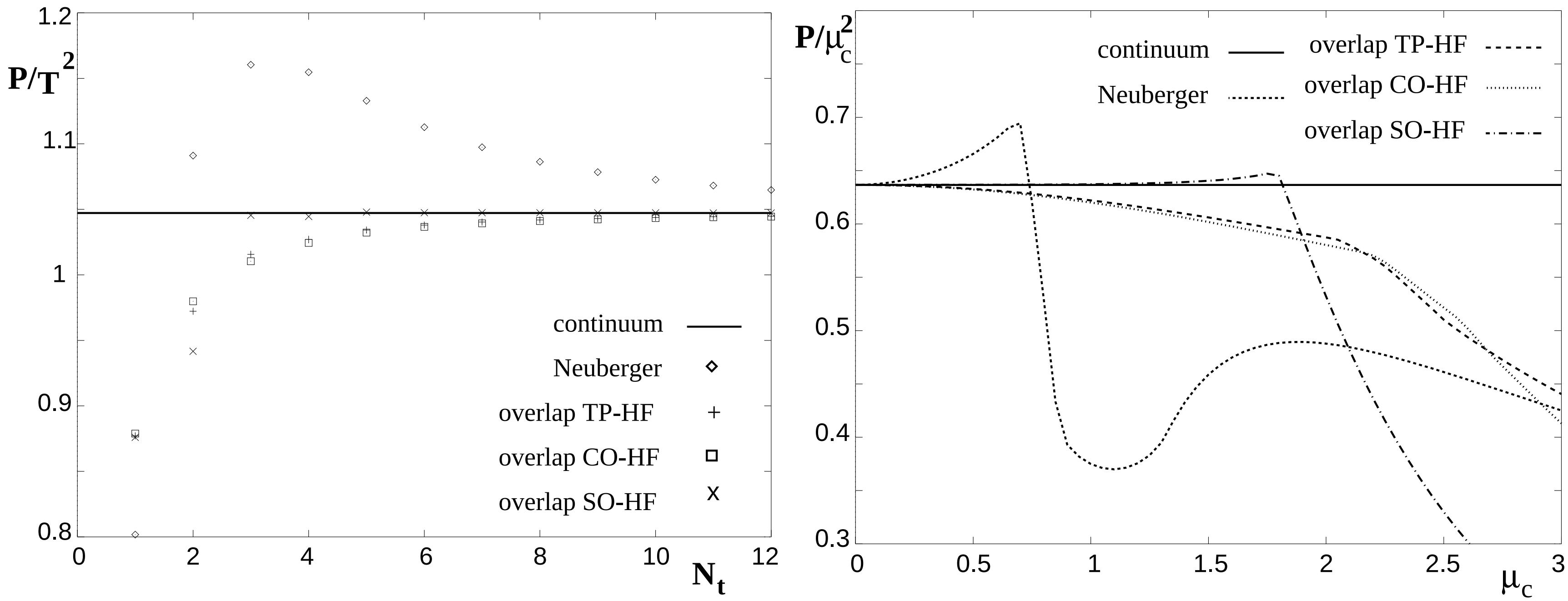

Thermodynamic scaling ratios pressure/(temperature)^2 *(left) and* pressure/(chemical potential)^2 *(right) for free 2d overlap fermions.*

The hierarchy of the scaling behavior is confirmed in all respects.

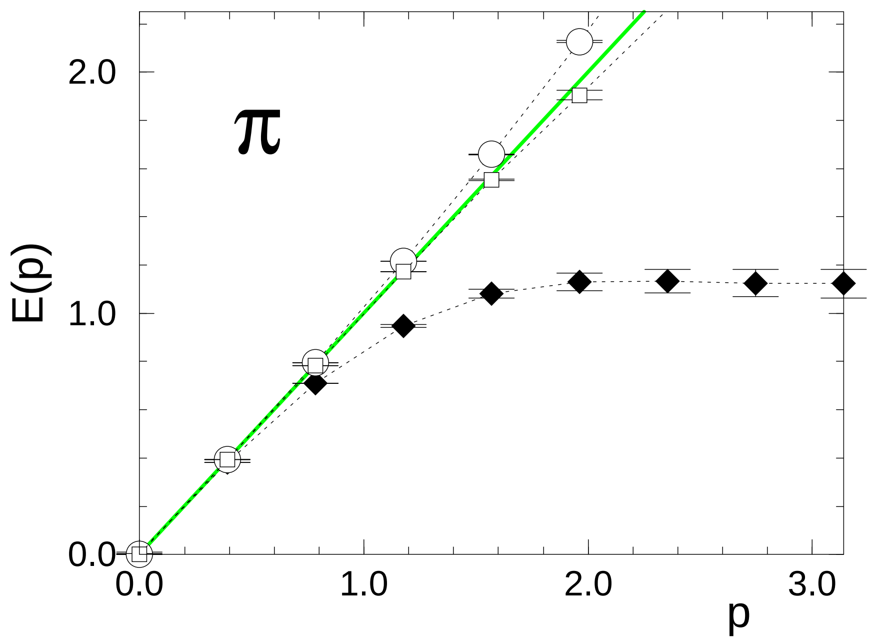

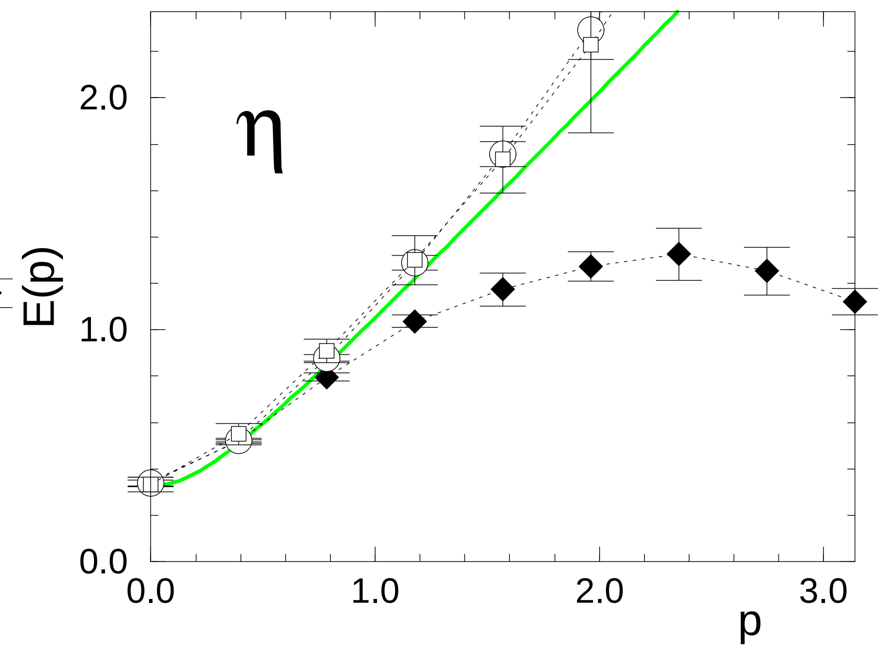

"Mesonic" dispersion relations in the Schwinger model with two types of overlap-HFs (open circles and squares).

Both the "pion" (left) and the "η-meson" (right) display a scaling which is far improved for the overlap-HFs compared to D_{N} (diamonds). [WB/Hip '00]

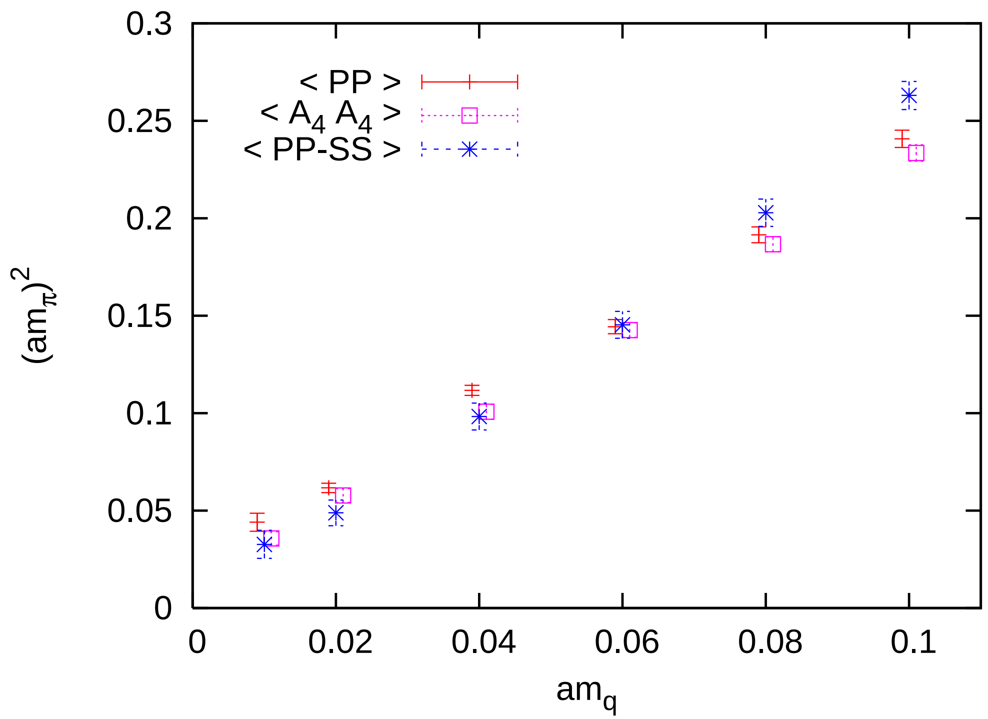

The pion mass evaluated from overlap-HFs in the p-regime of QCD in three different ways.

Follows the generic behavior $m_\pi^2 \propto m_q$ (m_q: light quark mass).

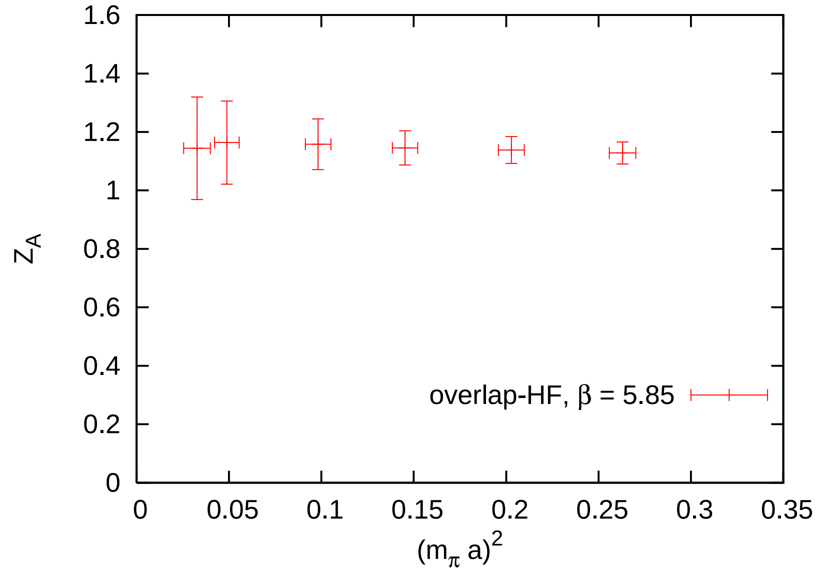

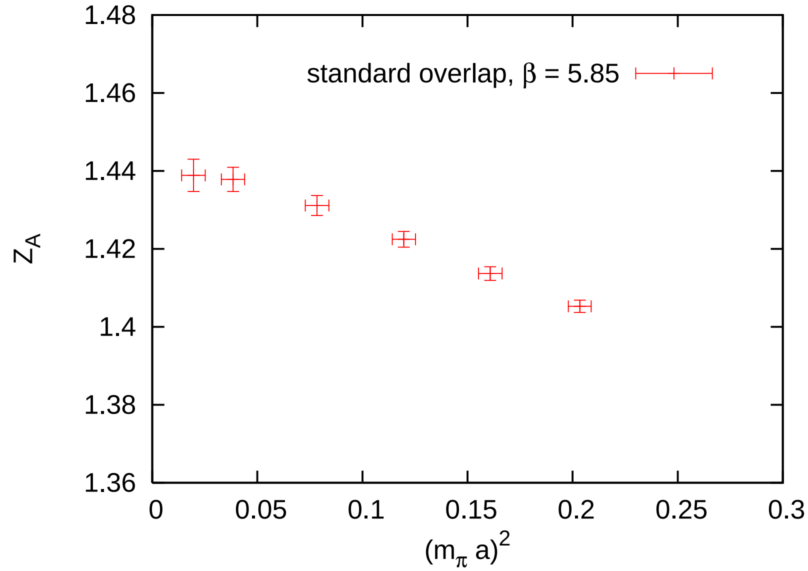

Axial current renormalization constant Z_A evaluated from PCAC relation, in QCD at $\beta = 5.85$.

For D_{ovHF} (left) we find $Z_A \approx 1$ [WB/Shcheredin '06], in contrast to the result with the Neuberger operator D_{N} (right) [WB et al. '04].

Topological charge: sound definition through the Index Theorem, but still depends on the choice of the Ginsparg-Wilson Dirac operator. [Hasenfratz/Laliena/Niedermayer '98]

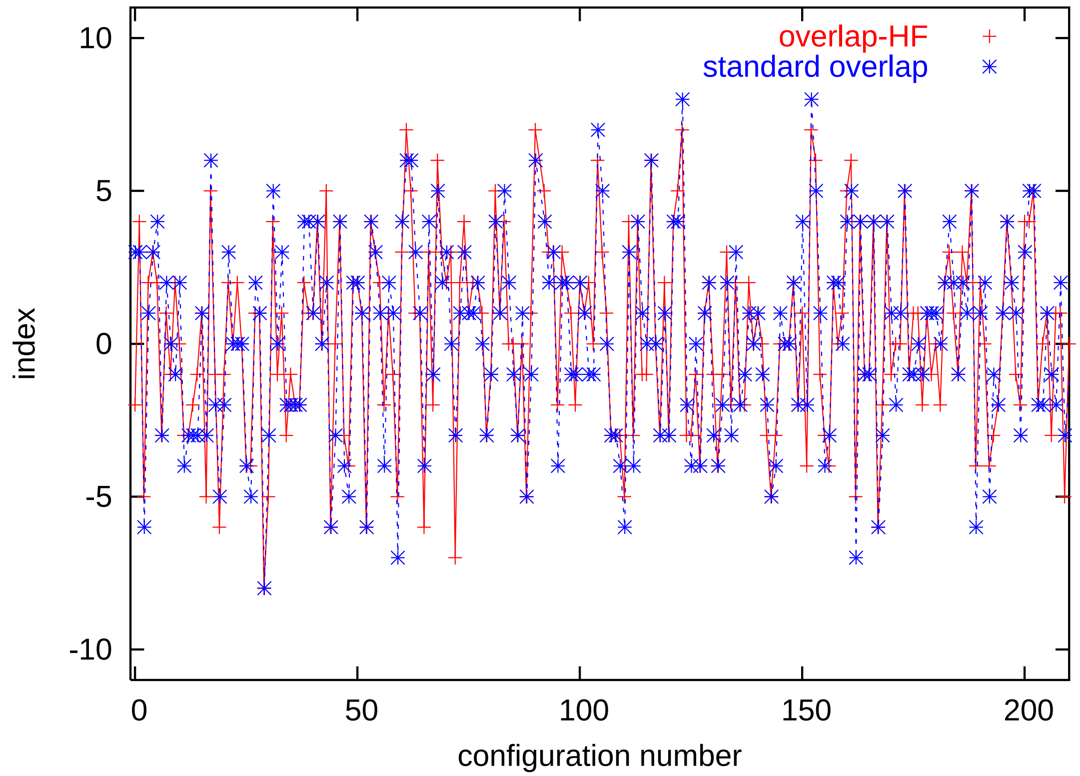

Index histories for D_{ovHF} and for D_{N} (at $\rho = 1.6$) for the same QCD confs (generated quenched at $\beta = 5.85$)

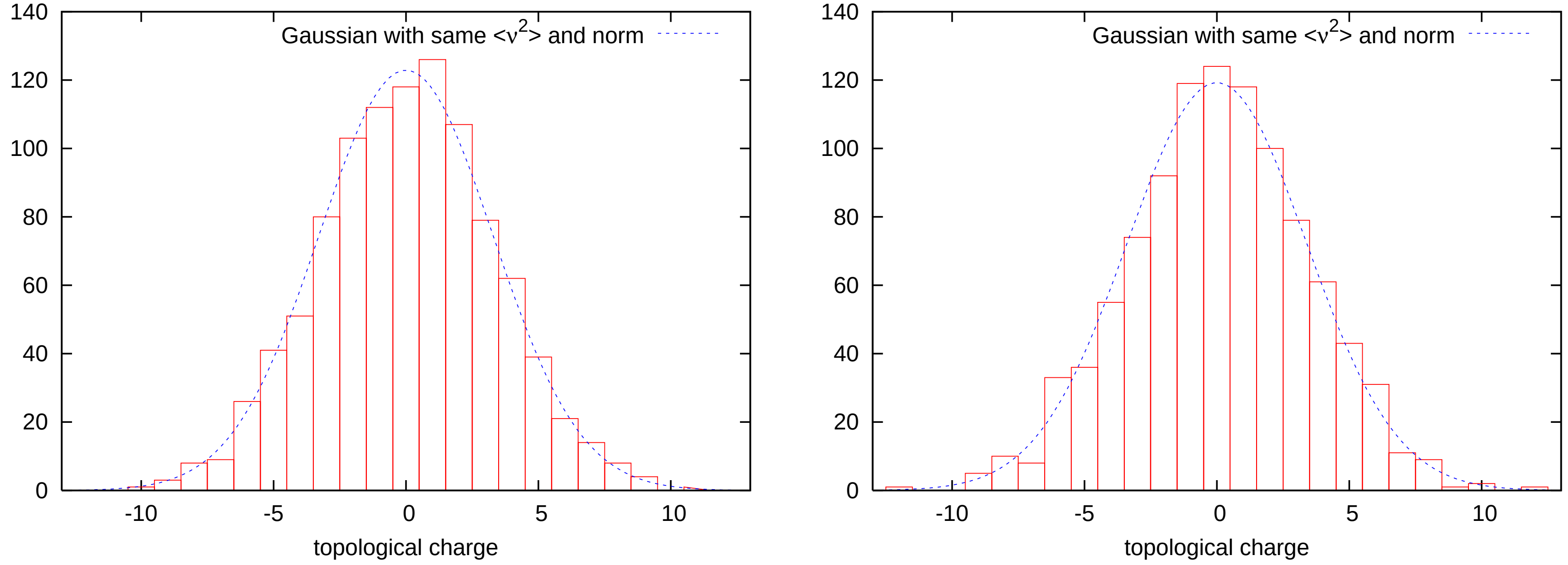

Histograms of $D_{\rm ovHF}$ *indices (left) and of* $D_{\rm N}$ *indices (right), on a* $12^3 \times 24$ *lattice in QCD at* $\beta = 5.85$ *(1013 configurations)*

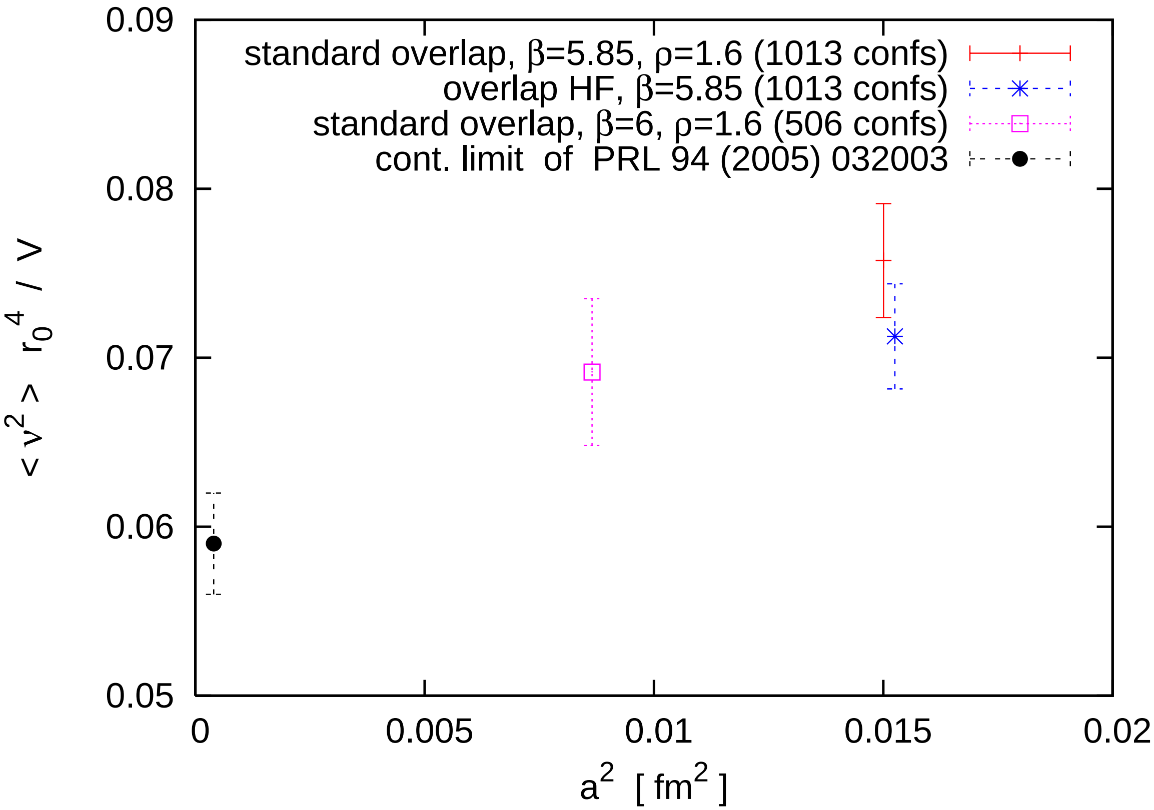

The topological susceptibility measured by indices of $D_{\rm ovHF}$ *and of* $D_{\rm N}$*, in a volume* $V = (1.48 \ {\rm fm})^3 \times 2.96 \ {\rm fm}$*, with two lattice spacings* a*.*

Our data [WB/Shcheredin '06] are consistent with the continuum extrapolation by Del Debbio/Giusti/Pica '05.

Roughly in agreement with Witten-Veneziano formula for $M_{\eta'}$.

Dirac spectrum and Random Matrix Theory (RMT)

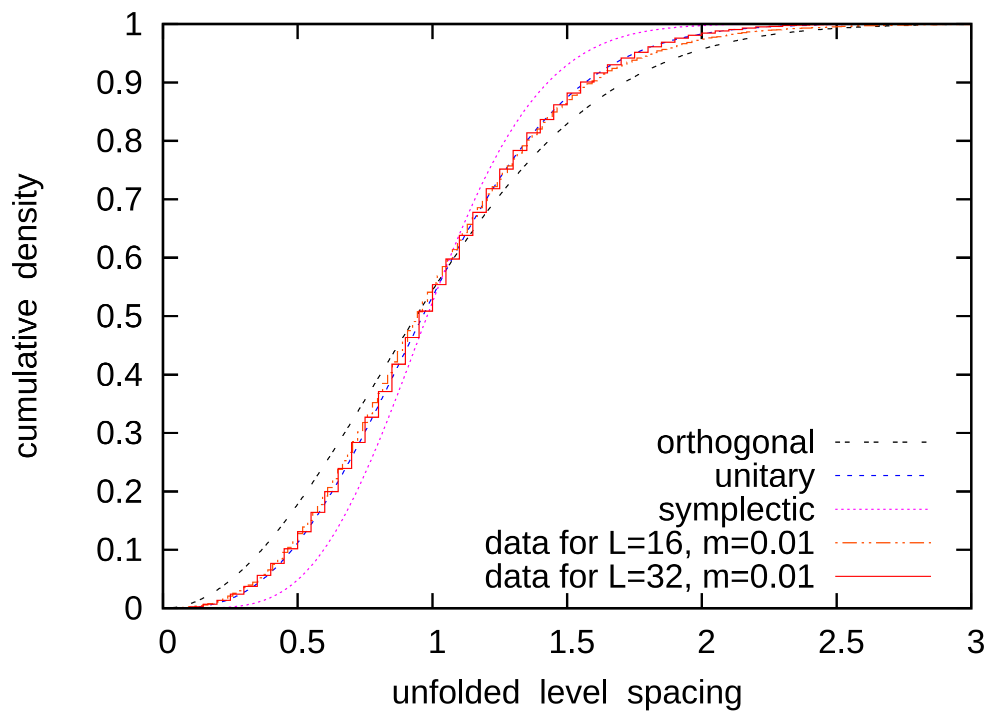

Cumulative density of the unfolded level spacing distribution.
RMT prediction for the orthogonal, unitary and symplectic ensemble.

Data from dynamical overlap-HF simulations in the Schwinger model at fermion mass $m = 0.01$: clear agreement with the unitary ensemble.
(For $L = 16$, slight deviation for level spacings $\gtrsim 1.5$. At $L = 32$, even that deviation disappears.) [WB/Hip/Shcheredin/Volkholz '12].

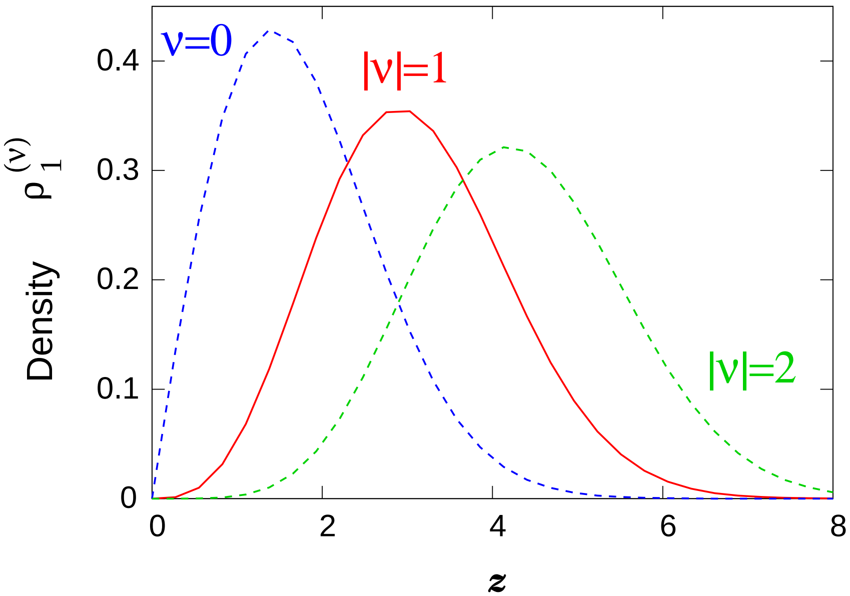

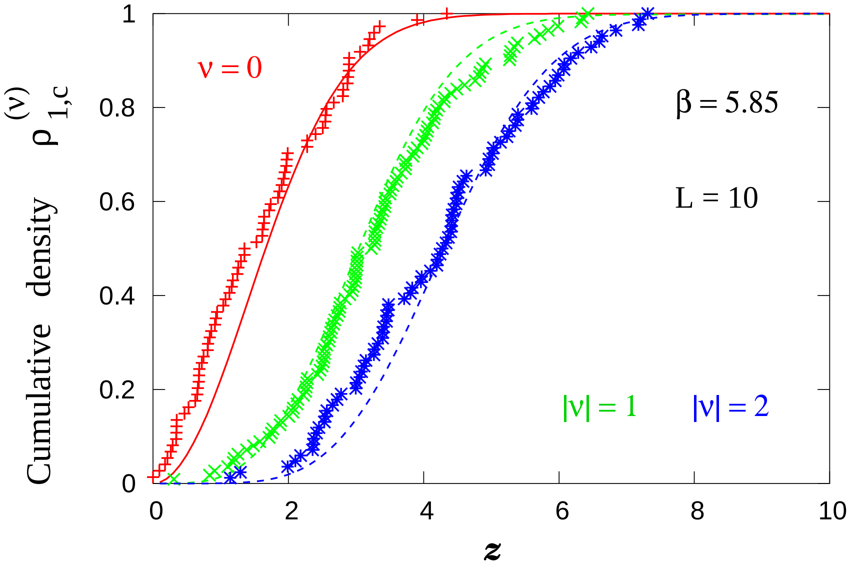

Left: RMT predictions for the **leading non-zero Dirac eigenvalue** in the topological sectors with charge $|\nu| = 0,\ 1$ and 2 $\ (z := \Sigma V \lambda_1)$.

Right: RMT predictions (lines) and simulation results for the corresponding **cumulative densities**. QCD data with $D_{\rm N}$ on a 10^4 lattice at $\beta = 5.85$ roughly follow the RMT predictions [WB/Jansen/Shcheredin '03].

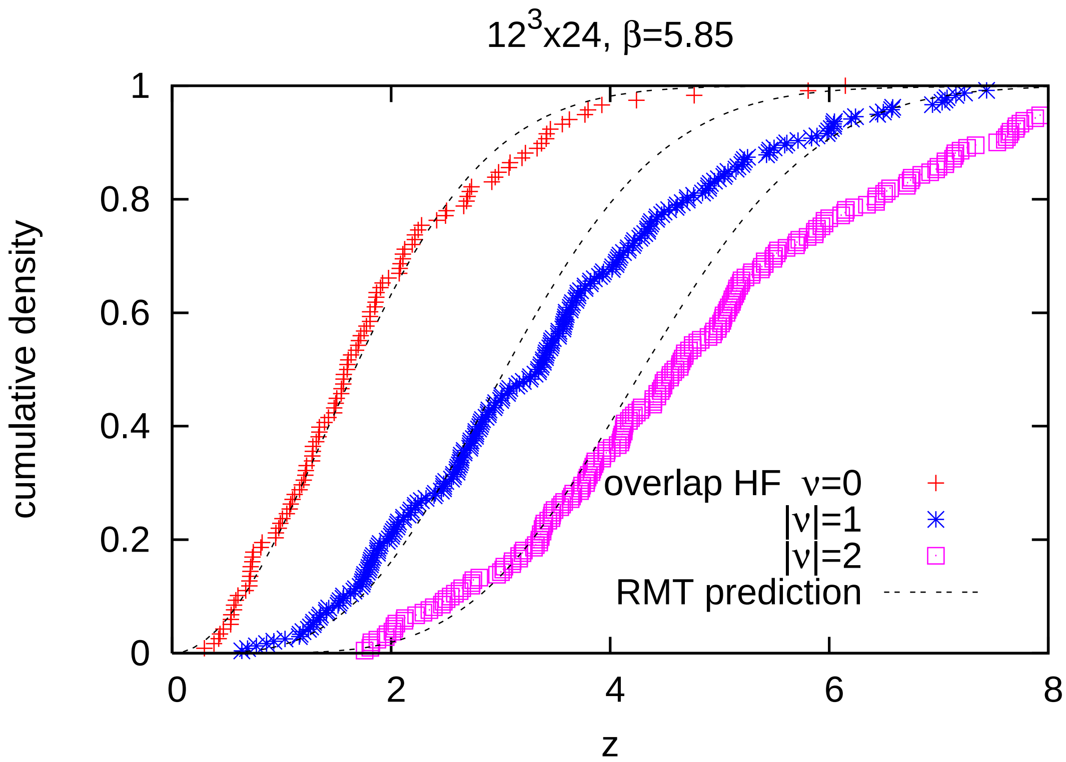

Cumulative density of the (Möbius projected) lowest Dirac eigenvalue λ_1 *of the overlap-HF operator, in the topological sectors* $|\nu| = 0,\ 1,\ 2.$

RMT predictions vs. data for $z = \Sigma V \lambda_1$ with $\Sigma^{1/3} = 298\ \mathrm{MeV}$ (optimal value in sector $\nu = 0$).

This value works well up to $z \lesssim 3$ in all topological sectors, well beyond the Thouless value $z_{\mathrm{Thouless}} \lesssim 1$, which is often considered a theoretical bound for the applicability of these predictions.

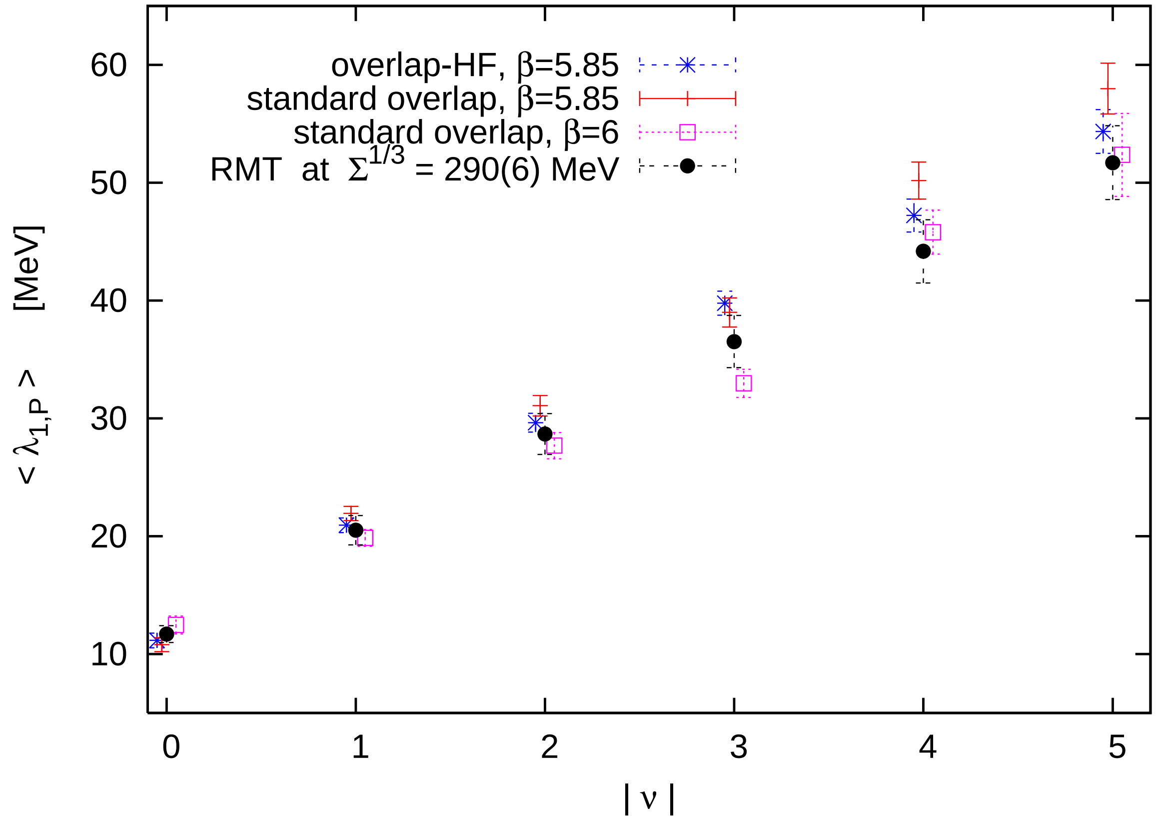

Mean values of the first non-zero Dirac eigenvalue (in physical units) in the charge sectors $|\nu| = 0 \ldots 5$.

All data are compatible with chiral RMT, if we choose
$\Sigma^{1/3} = 290(6)\ \mathrm{MeV}$ [WB/Shcheredin '06]

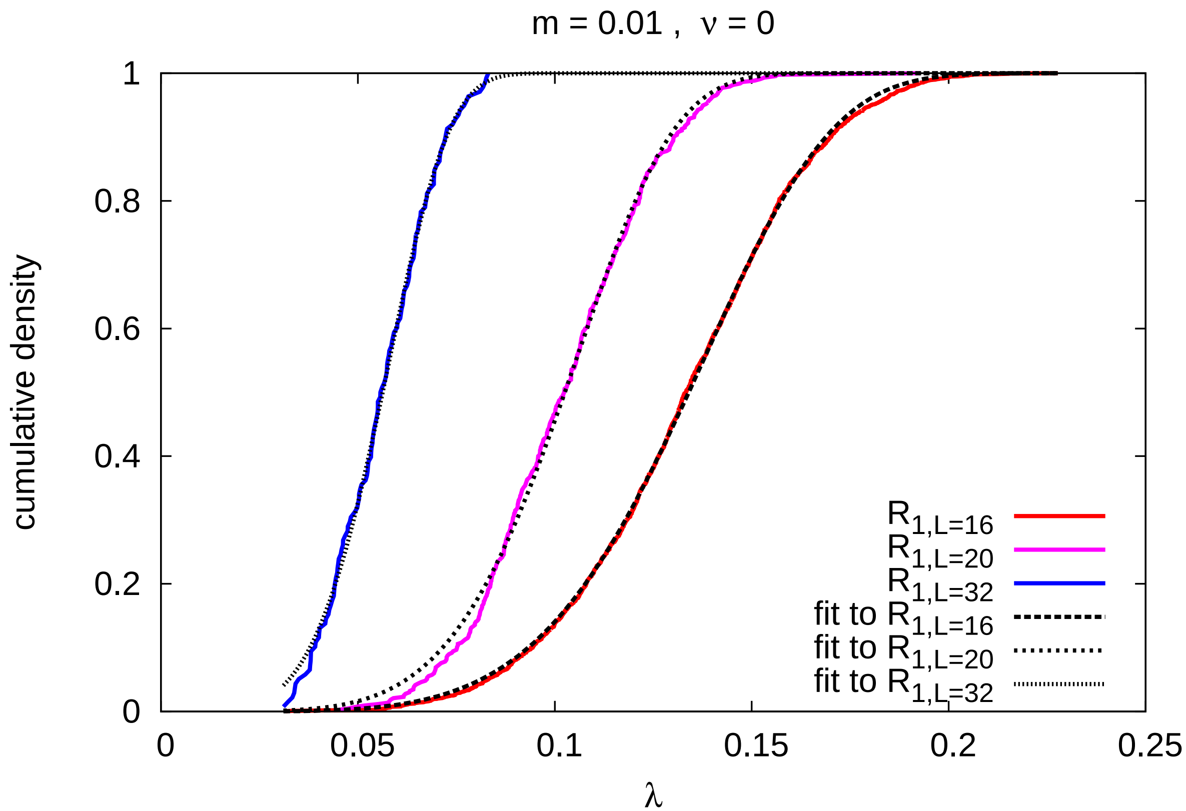

Cumulative density of λ_1 of $D_{\rm ovHF}(m = 0.1)$ in the 2-flavor Schwinger model, at topological charge $\nu = 0$, on square lattices of size $L = 16$, 20 and 32, $\beta = 5$.

Excellent agreement with a prediction by T. Kovács' of a decoupled — and therefore **Poisson distributed** — leading eigenvalue, due to $\Sigma(m = 0) = 0$ ($\Sigma \propto m^{1/\delta}$, $\delta = (N_{\rm f} + 1)/(N_{\rm f} - 1)$) [Landa-Marbán/WB/Hip '13]

Schwinger model in the “δ-regime”: $L_t \gg L$

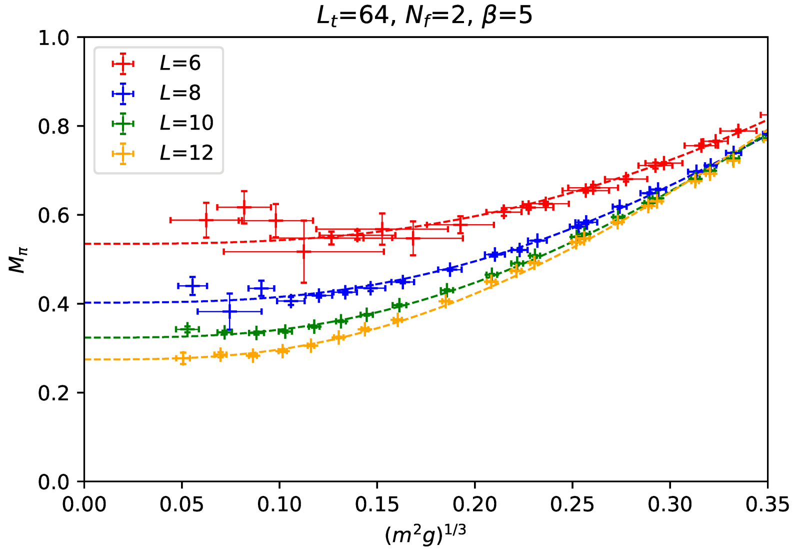

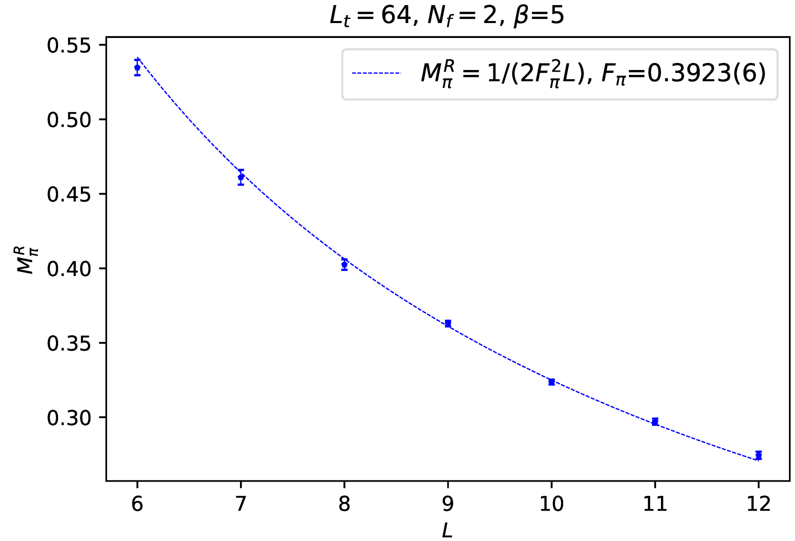

Left: “Pion” mass M_π with dynamical Wilson fermions. For small fermion mass m (determined by the PCAC relation) and small spatial extent L: significant errors. Still, the full range enables sensible extrapolations to the residual “pion” mass M_π^{R} in the chiral limit.

Right: Residual “pion” masses M_π^{R}, extrapolated to $m = 0$, at $L = 6 \dots 12$. The data follow a fit $\propto 1/L$.

Assuming $M_\pi^{\mathrm{R}} = 1/(2F_\pi^2 L)$ *yields* $F_\pi := 0.3923(6)$ (dim’less in $d = 2$)

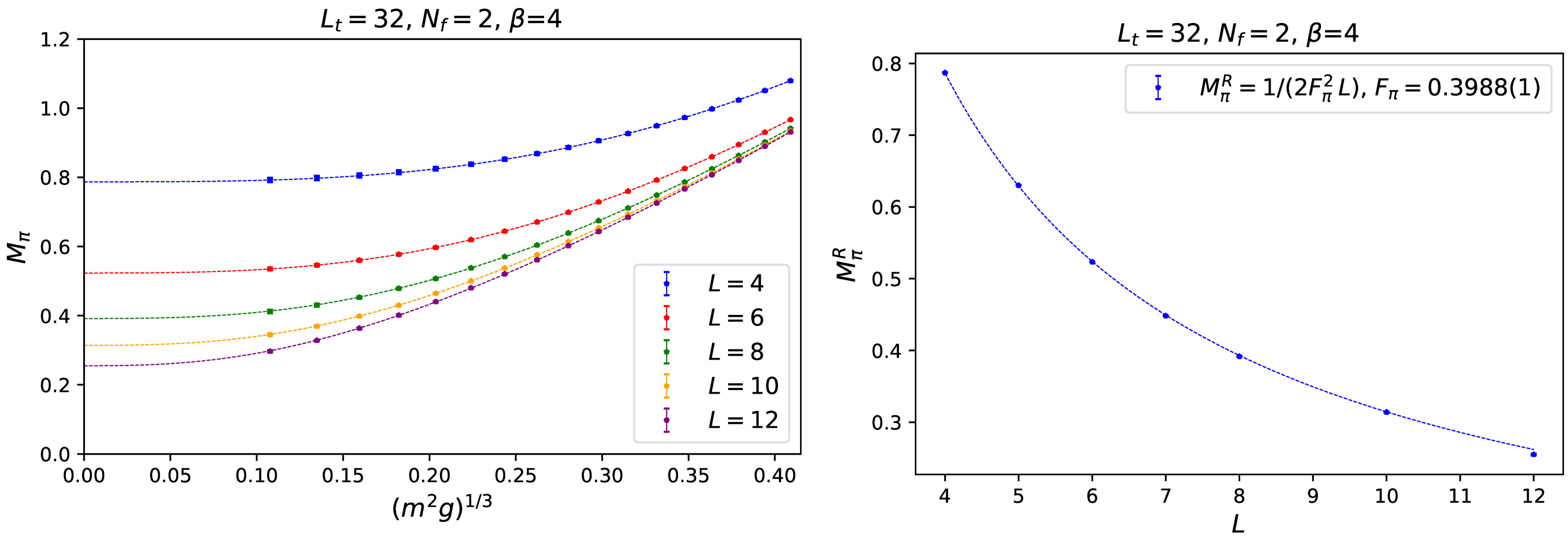

Left: Like previous figure, but M_π measured with the overlap-HF, using quenched, re-weighted confs. Smooth chiral extrapolations for all spatial sizes $L = 4 \dots 12$.

Right: Again the fit $M_\pi^{\mathrm{R}} \propto 1/L$ works for $L < 12$, and leads to $F_\pi = 0.3988(1)$.

Well compatible with further results that we obtained for F_π by employing different methods, and in perfect agreement with $F_\pi = 1/\sqrt{2\pi} \simeq 0.3989 \dots$

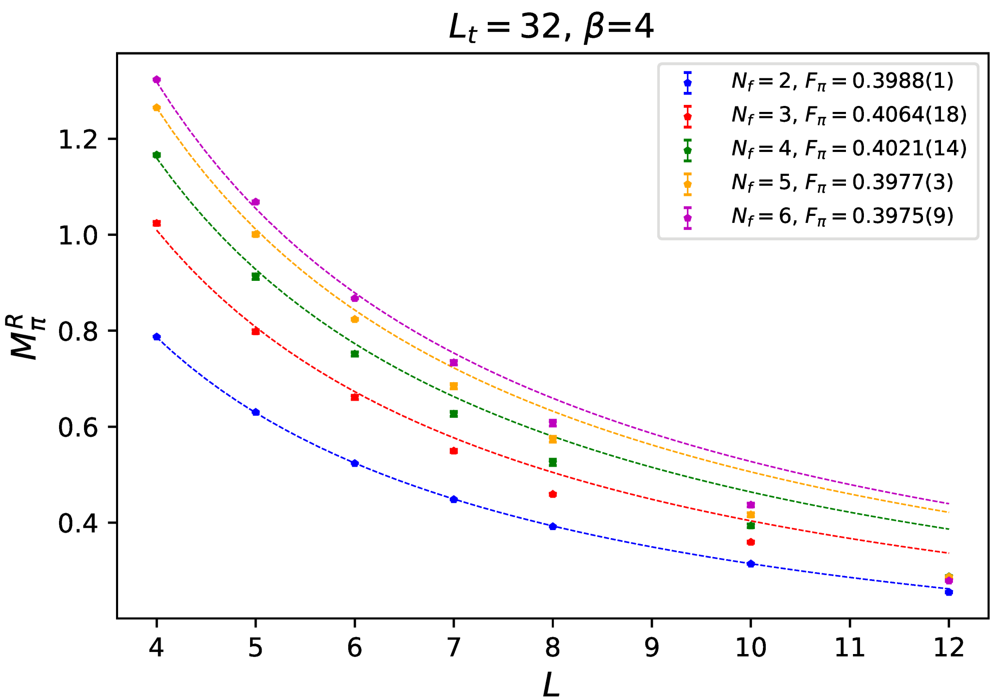

Residual "pion" masses $M_\pi^{\rm R}$ in the δ-regime ($L_t = 32$) for a variety of spatial sizes $L \ll L_t$, and $N_{\rm f} = 2 \dots 6$ flavors.

Chiral extrapolations of quenched, re-weighted results with the overlap-HFs at $\beta = 4$. (Fits in the range where they are successful).

Consistent values for F_π with the effective formula

$$M_\pi^{\rm R} = \frac{N_\pi}{2F_\pi^2 L} \, , \quad N_\pi = \frac{2(N_{\rm f} - 1)}{N_{\rm f}}$$

The value $F_\pi(m=0) = 1/\sqrt{2\pi} = 0.3989\ldots$

is consistent with the 2d Gell-Mann–Oakes–Renner Relation

$$\Sigma \;=\; -\langle\bar{\psi}\psi\rangle = \frac{M_\pi^2}{4\pi m} \qquad (\text{Smilga }'92,\ \text{Hetrick/Hosotani/Iso }'95)$$

$$F_\pi^2(m) \;=\; \frac{2m\Sigma}{M_\pi^2} \quad\Rightarrow\quad F_\pi = \frac{1}{\sqrt{2\pi}}\ ,$$

and with the Witten-Veneziano Formula

$$M_\eta^2 = \frac{N_\mathrm{f}\, g^2}{\pi} \stackrel{!}{=} \frac{2N_\mathrm{f}\chi_\mathrm{t}^\mathrm{q}}{F_\eta^2} \quad \text{and} \quad F_\pi = F_\eta\ ,$$

where $\chi^\mathrm{q} = g^2/4\pi^2$ (Seiler/Stamatescu '87) is the quenched, topological susceptibility. [Nieto Castellanos/Hip/WB, in prep.]

Matches light-come study of $\langle 0|\partial_\mu J_\mu^5(0)|\pi(p)\rangle = M_\pi^2 F_\pi \to F_\pi \simeq 0.3945$ [Harada et al. '94], but not $\langle 0|J_\mu^5(0)|\pi(p)\rangle = \mathrm{i}p_\pi^2 F_\pi = 0$ [Dürr]

Overview

- **Truncated perfect hypercube fermion (HF)**

  Ultralocal, good scaling, approx. rotation symmetry

- **Overlap-Hypercube fermion (Overlap-HF)**

  High degree of locality, valid up to strong gauge coupling
  low condition number of $A^\dagger A$
  good scaling and approx. rotation symmetry inherited from HF

In both cases:

Some additional effort to implement and simulate, but feasible.

Variety of favorable properties, somewhat forgotten in recent years (even by myself), deserves more attention.